AUBURN UNIVERSITY

SAMUEL GINN
COLLEGE OF ENGINEERING

**Research Report**

# Distortion Induced Fatigue of Horizontally Curved Steel Girders

*Submitted to the*

Highway Research Center

*Prepared by*

Sayed Mohamad Jalali Moghadam

Aditya Rajesh Shah

James S. Davidson

**June 2020**

Highway Research Center
Harbert Engineering Center
Auburn, Alabama 36849

www.eng.auburn.edu/research/centers/hrc.html

| | | |
|---|---|---|
| **1. Report No.**<br>IR 17-01 | **2. Government Accession No.** | **3. Recipient Catalog No.** |
| **4. Title and Subtitle**<br><br>Distortion Induced Fatigue of Horizontally Curved Steel Girders | | **5. Report Date**<br>06/10/2020<br><br>**6. Performing Organization Code** |
| **7. Author(s)**<br>S.M. Jalali Moghadam, Aditya Rajesh Shah and James S. Davidson | | **8. Performing Organization Report No.**<br>IR 17-01 |
| **9. Performing Organization Name and Address**<br>Highway Research Center<br>Department of Civil Engineering<br>238 Harbert Engineering Center<br>Auburn, AL 36849 | | **10. Work Unit No. (TRAIS)**<br><br>**11. Contract or Grant No.** |
| **12. Sponsoring Agency Name and Address**<br>Highway Research Center<br>Department of Civil Engineering<br>238 Harbert Engineering Center<br>Auburn, AL 36849 | | **13. Type of Report and Period Covered**<br><br>**14. Sponsoring Agency Code** |
| **15. Supplementary Notes** | | |


**16. Abstract**

The overall objective of this study was to define the mechanisms that could cause fatigue cracks in curved steel bridge girders with slender webs. A comprehensive literature review of curved girder fatigue studies was conducted that confirmed that only a couple of studies have been conducted on this topic, which were several decades ago. Approaches for analyzing stress concentrations in curved girder systems using finite element were investigated, which led to the adoption of a sub-modeling simulation technique that was applied to investigate the web performance at the transverse stiffeners connection to the bottom flange where the lateral displacements were restrained. The analyses indicated that there is significant potential that fatigue cracks will occur at the web to transverse stiffener connection near the bottom flange.



| | | | |
|---|---|---|---|
| **17. Key Words**<br>curved girder, slender web, fatigue design, finite element analysis | | **18. Distribution Statement**<br>No restrictions. | |
| **19. Security Classification (of this report)**<br>Unclassified | **20. Security Classification (of this page)**<br>Unclassified | **21. No. of pages**<br>66 | **22. Price** |

**Research Report**

# Distortion Induced Fatigue of Horizontally Curved Steel Bridges

*Submitted to the*

Highway Research Center

*Prepared by*

S.M. Jalali Moghadam
Aditya Rajesh Shah
James S. Davidson

**June 2020**

# DISCLAIMERS

The contents of this report reflect the views of the authors who are responsible for the facts and accuracy of the data presented herein. The contents do not necessarily reflect the official views or policies of Auburn University or the Highway Research Center. This report does not constitute a standard, specification, or regulation. Comments contained in this report related to specific testing equipment and materials should not be considered an endorsement of any commercial product or service; no such endorsement is intended or implied.

NOT INTENDED FOR CONSTRUCTION, BIDDING, OR PERMIT PURPOSES

S.M. Jalali Moghadam
Aditya Rajesh Shah

*Research Supervisor*
James S. Davidson

# ACKOWLEDGEMENTS

This project was sponsored by the Highway Research Center at Auburn University.

# ABSTRACT

Longer span lengths and faster erection make horizontally curved steel bridges an attractive choice for highway flyovers compared to concrete bridges. However, the mechanical behavior of curved steel girder superstructures is complex. Curved girders experience high torsion and warping under the applied loads. The web of the slender curved girders may undergo large lateral deformations. The combined effect of bending stresses and web deformations can cause high secondary stresses at the web boundaries. In addition, the restrained lateral translations at the bracing connections can cause stress concentrations that are added to significant stresses that are locked in during fabrication and erection. While these stresses may not significantly influence the nominal bending strength definition used in bridge design, the resulting fatigue crack potential could affect service life and future maintenance costs. The overall objective of the study was therefore to define the mechanisms associated with fatigue cracks that could occur in curved steel bridge girders with slender webs. A comprehensive literature review of curved girder fatigue studies was conducted that confirmed that only a couple of studies have been conducted on this topic, which were several decades ago. Approaches for analyzing stress concentrations in curved girder systems using finite element were investigated, which led to the adoption of a sub-modeling simulation technique that was applied to investigate the web performance at the transverse stiffeners connection to the bottom flange where the lateral displacements were restrained. The analyses indicated that there is significant potential that fatigue cracks will occur at the web to transverse stiffener connection near the bottom flange.

# TABLE OF CONTENTS

# LIST OF FIGURES

# LIST OF TABLES

Chapter 1

# Introduction

## 1.1 Problem Overview

Horizontally curved steel bridges provide economical design benefits, span long distances, have shallow depth, and are more aesthetically pleasing than concrete bridges. These structures are the dominant choice for curved highway bridges and comprise approximately thirty percent of all U.S. steel bridges (Zureick et al. 2000). Large scale research efforts were initiated in the 1970s and continued into 1990s to investigate behavior of curved steel girder and to develop design guidelines and recommendations (Consortium of University Research Teams 1975; Zureick, Naqib, and Yadlosky 1994; Structural Stability Research Council (SSRC) Task Group 14. 1991). Recently, numerous studies were carried out to further investigate the effect of curvature on the stability and strength of slender curved girders for more liberal design considerations (Issa-El-Khoury, Linzell, and Geschwindner 2014; Frankl and Linzell 2017; Broujerdian, Mahyar, and Ghadami 2015; Sanchez and White 2012). Although the stability and strength of curved steel girders have been comprehensively researched, their design for fatigue is still based on straight girder characteristics.

## 1.2 Objectives

The overall objective of the study was to define mechanisms that could lead to fatigue problems in the girders of horizontally curved steel bridge superstructures. The following tasks were done to achieve the aim:

- Review the mechanics of curved girder systems;
- Define the fatigue problem mechanisms in slender straight and curved girders based on prior research by others;
- Determine finite element modeling approaches that can be used to analyze the fatigue characteristics curved bridge girders.

### 1.3 Report Organization

Chapter 2 presents the mechanics of curved girders and how the applied vertical loads affect the resulted stress components. A brief background of specific curved girder stresses is given at the beginning, followed by a guide specification development review. The stability of the flange and web of the curved I-girders is then reviewed and the V-load method of analysis is explained.

Chapter 3 discusses relevant fatigue assessment methods, including nominal-stress, hot-spot stress, and the linear elastic fracture mechanic (LEFM) method. Finally, residual stress effect on fatigue life of steel structures is presented.

Chapter 4 addresses fatigue problems associated with straight multiple girder systems and slender girders. Distortion induced fatigue and web breathing are discussed, and fatigue studies specific to curved girders are reviewed. Current fatigue design limits related to each type of fatigue problems are also presented.

Chapter 5 presents the development of the finite element modeling approach. Two modeling strategies developed to capture the potential fatigue cracking regions are explained and the results are discussed.

Chapter 6 presents the summary, conclusions and recommendations resulting from the project.

Chapter 2

# Curved Girder Mechanics

## 2.1 Background

Curved girders experience torsional load upon receiving the vertical loading due to curvature that adds complexity to analysis and design compared to straight girders (Culver and Nasir 1969). Curved girder cross-section normal stress components are due to bending, lateral (radial) bending, warping and distortional stresses; shear stresses include uniform (St. Venant) and non-uniform torsion, as illustrated in Figure 2.1 (Schuenzel 1982). Extensive research has been carried out to study the effect of these stresses on the behavior of curved girders. After a brief timeline describing the research events that took place in the field of horizontally curved bridges, additional discussion of these investigations is provided.

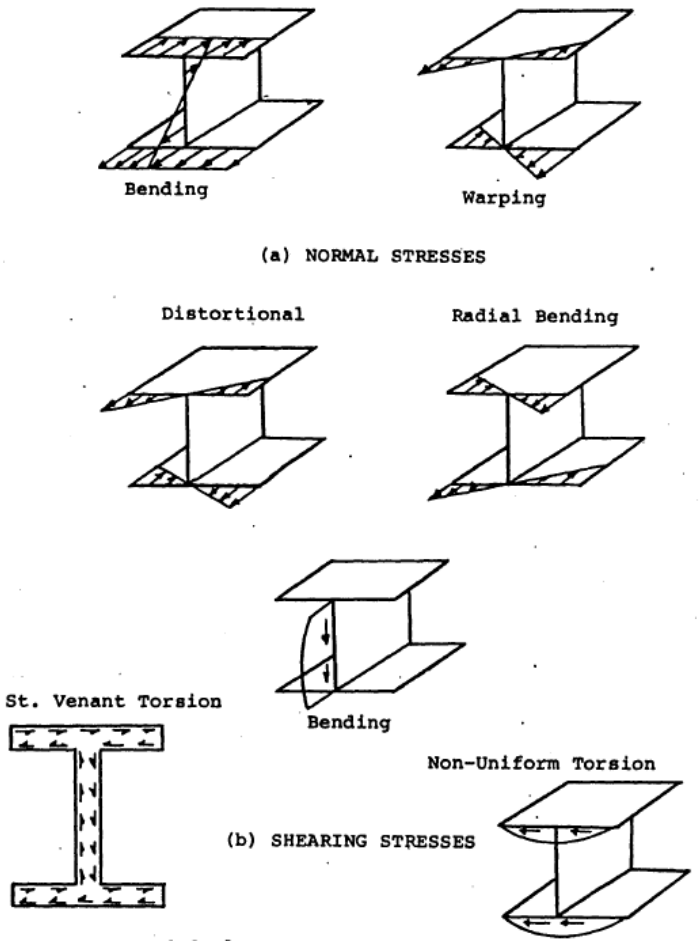


**Figure 2.1 Curved girder stress distributions (Schuenzel 1982)**

## 2.2 Guide Specification Development Review

Before the mid-1960s, research on the behavior of horizontally curved girders was limited to theoretical work based on the linear elastic static behavior of curved elements. The earliest work on curved beam theory attributed by St. Venant (1843) over 170 years ago (Ziemian 2010). The initial step toward developing a guide specification for designing the curved bridges started by the Consortium of University Research Teams (CURT) project in 1969. The CURT project was managed by the Federal Highway Administration (FHWA) and supported by 25 states. The CURT project aimed at a) reviewing published materials related to curved bridges; b) running experimental and analytical analysis

applying the knowledge of curved bridge design; c) investigating the other state corporation findings; d) developing the simple design and analysis methods; and e) verifying the recommended design and analysis methods with the acquired analytical and experimental data (Linzell, Hall, and White 2004).

Four universities, namely, the University of Rhode Island, Syracuse University, the University of Pennsylvania, and Carnegie-Mellon University, participated in the CURT project. The University of Rhode Island conducted full-scale tests on two single scale curved boxed girders (Stegmann and Galambos 1976). A modified grid method of analysis, taking into consideration non-uniform torsion, was used to determine stresses (Schuenzel 1982). The University of Pennsylvania conducted small scale model tests using rolled beams (Stegmann and Galambos 1976). Non-uniform torsion was neglected while calculating stresses on the cross section (Schuenzel 1982). Hence, the method of analysis was not accurate. Syracuse University used a three-dimensional method of analysis of a scaled model of composite curved plate girder (Stegmann and Galambos 1976). The analysis assumed the effects of warping torsion and assumed that all members are straight and full composite action would be achieved. Charles Culver at Carnegie-Mellon investigated the limit states of horizontally curved girders (Schuenzel 1982). The investigation included studies of web shear, local and lateral buckling of compression flange, combined bending and shear failure, and web buckling. Carnegie-Mellon conducted an extensive testing program to test the strength of curved girders.

Based on the analytical and experimental studies carried out by the universities under CURT, a tentative design specification for horizontally curved girders was developed in 1978 (Galambos 1978). This specification was based on allowable stress design considering only the elastic behavior (Schuenzel 1982). Later, Load Factor Design (LFD) criteria were added to the specifications through a research project sponsored by the American Iron and Steel Institute (AISI) in the mid-1970s (Stegmann and Galambos 1976).

The research done under CURT along with other important investigations resulted in the development of AASHTO Guide Specifications of Horizontally Curved Bridges (AASHTO 1993). However, the Guide Specifications were disjointed and difficult to follow. There was a significant discontinuity in the compressive strength formulations for non-compact and compact sections (Davidson and Yoo 2000). Moreover, the value of strength calculated by strength predictor equations for curved sections did not approach that predicted by straight girder equations when the radius of curvature approached infinity (Davidson and Yoo 2000). For these reasons, among others, it was not adopted as an integral part of the AASHTO Standard Specifications for Highway Bridges (AASHTO 1992).

In 1992, the Federal Highway Administration (FHWA) initiated the Curved Steel Bridge Research Project (CSBRP) to understand the fundamental behavior of horizontally curved bridges that would lead to the development of LRFD specifications for curved bridge design (Ziemian 2010). Following the CSBRP, a significant amount of research was undertaken to study the behavioral characteristics of curved girders. Strength predictor equations were developed involving a number of design issues like the curvature effect on the lateral buckling strength of curved girder over straight girders, strength reduction of web panels due to curvature under pure bending and combined bending and shear, inelastic behavior of horizontally curved girders, etc. (Davidson and Yoo 2000). The work of CSBRP was extended in 1999 through a project that was jointly sponsored by FHWA and the American Iron and Steel Institute (AISI) that used the nonlinear finite element analysis to expand the knowledge gained from experimental tests conducted under CURT and CSBRP projects (Ziemian 2010). This analytical work resulted in the unification of the design equations for straight and curved steel girders into the 2004 AASHTO LRFD Design Specifications.

## 2.3 Stability of Curved I-girders

### 2.3.1 Curvature Effects on Flange Behavior

For straight I-shaped plate girders, the primary role of the web in the high moment region is to maintain relative distance between the flange plates. Therefore, the efficient design of plate girders requires the flanges to carry the primary moment and the webs to be designed as slender. Thus, the nominal moment strength of straight, slender plate girders is controlled either by the limit state of yielding of the tension flange or buckling of the compression flange. Inelastic behavior of webs is not considered (Davidson, Ballance, and Yoo 1999). However, for curved girders, the presence of curvature greatly complicates the behavior and design considerations. Curvature induces both warping torsion in the cross-section, and transverse displacement of the web (Davidson, Ballance, and Yoo 1999). To account for the effect of curvature on the flexure resistance contributed by the flanges, the normal stress acting on a flange is approximated as the linear addition of the bending normal stress and the normal stress resulting from the lateral bending of the flange, as illustrated in Figure 2.2. The sources of lateral bending stress are associated with either non-uniform torsion or the lateral force acting on the girder (Ziemian 2010).

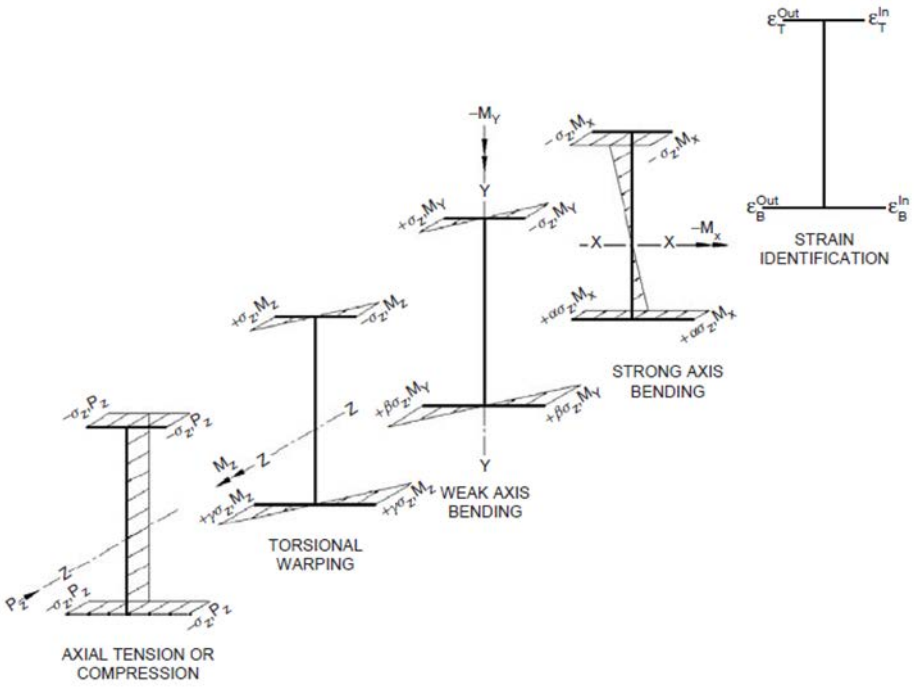


**Figure 2.2 Components of longitudinal stress (Hartmann 2005)**

As the curvature is increased, the membrane stress distribution becomes increasingly nonlinear through the depth of the section (Davidson, Ballance, and Yoo 1999). Because of this reduction of membrane stress along the web, the flanges carry a higher load. Thus, even without considering the warping stress resulting from curvature, the curved section would be unable to carry an equal magnitude of vertical moment as compared to the similar straight section before the yielding of the flanges initiates.

Culver and Nasir (1969) investigated the local buckling of curved girder flanges in both elastic and inelastic range to determine the governing differential equation. Shear stresses were neglected and the maximum bending and warping stresses were conservatively assumed to occur at the same point along the girder. The slenderness requirement generated from the characteristic equation is as follows (Culver and Nasir 1969):

$$\frac{b}{t} = \frac{k\,E}{12\left(1-\upsilon^2\right)F_y} \tag{2.1}$$

Where $b$ = width of the flange, $t$ = thickness of flange, $E$ = modulus of elasticity, $F_y$ = yield stress, and $k$ = buckling coefficient. For uniform stress (bending only), curvature had minimal effect on the value of $k$. For non-uniform stress, warping and bending, the value of $k$ significantly reduced depending on the yielding of the flange, making the flanges more compact.

Davidson and Yoo (1996) showed that there is a reduction in elastic buckling strength of the curved compression flanges due to the warping stress gradient acting across the flanges. The primary factors that contributed to this reduction were $f_w / f_b$ ratio in the compression flange and the relative boundary condition provided by the web to the flanges. The effect of the curvature was given by:

$$(\sigma_{cr})_{cv} = (\sigma_{cr})_{st}\left[1.0643 - \frac{0.15}{0.35}\frac{f_w}{f_b}\right] \tag{2.2}$$

Where $(\sigma_{cr})_{cv}$ = critical stress for curved girder; $(\sigma_{cr})_{st}$ = critical stress for straight girder; $f_w$ = warping stress; and $f_b$ = bending stress.

One of the challenges of designing the curved girders was how to relate the combination of lateral bending stress and normal bending stress to flange bending resistance. Hall (1998) proposed a unified approach, known as the "1/3rd rule" that applies to both tangent and curved I-girder bridges. The 1/3rd rule was first introduced into the 2004 AASHTO Load and Resistance Factor Design (LRFD) and is given by:

$$f_{bu} + \frac{1}{3} f_l \le \phi_f F_{nc} \tag{2.3}$$

where $f_{bu}$ = flange stress calculated without consideration of flange lateral bending; $f_l$ = flange lateral bending stress; $\phi_f$ = resistance factor for flexural; $F_{nc}$ = nominal flexural resistance of the flange.

### 2.3.2 Curvature Effects on Web Behavior

As mentioned in the previous section, curvature induces warping of the cross-section, and, more importantly, for the web consideration, transverse displacement of the web, which induces through the thickness stresses in the girder that decrease the moment carrying capacity of the girder. The curvature also causes nonlinear distribution of membrane stress throughout the depth of the web. This distribution becomes increasingly nonlinear with the increase in curvature, which results in an increase in normal stress in the flanges, thus effectively reducing the moment carrying capacity of girders (Davidson, Ballance, and Yoo 1999; Ziemian 2010).

Based on analytical and numerical research on curved girders, Culver (1972) developed an equation for the reduction in the slenderness of the web with no longitudinal stiffeners by modeling the web as a series of isolated cylindrical strips subjected to fictitious radial loading and "spring foundation" boundary condition. This equation was first used in the "Load Factor Design" of the Guide Specifications (Davidson, Ballance, and Yoo 1999). The web slenderness requirement developed is as follows:

$$\frac{D}{t_w} = \frac{36500}{\sqrt{F_y}}\left[1 - 8.6\frac{a}{R} + \left(\frac{a}{R}\right)^2\right] \tag{2.4}$$

where $D$ = depth of flange; $t_w$ = thickness of the flange; $F_y$ = yield stress; $a$ = panel length or distance between transverse stiffeners; and $R$ = radius of curvature at the center of panel.

Culver et al. (1973) published an improved version of his work a year later in which he modeled the girder by treating it as a two-way shell rather than as an individual strip (i.e., providing longitudinal stiffeners). The proposed equation was used in the "Allowable Stress Design" of the Guide Specifications. The equation

developed for curved girder web slenderness with longitudinal stiffeners is as follows:

$$\frac{D}{t_w} = \frac{46000}{\sqrt{f_b}}\left[1 - 2.9\sqrt{\frac{a}{R} + 2.2\frac{a}{R}}\right] \tag{2.5}$$

where $D$ = depth of flange; $t_w$ = thickness of the flange; $f_b$ = bending stress; $a$ = panel length or distance between transverse stiffeners; and $R$ = radius of curvature at the center of panel.

Daniels and Herbein (1980) conducted a five-year experimental project on the fatigue behavior of horizontally curved bridges at Lehigh University. New limitations were developed for the slenderness of webs in curved girders, stating that the slenderness limitations developed by Culver (1972) were too conservative (Ziemian 2010). The recommended equations published in the "Load Factor Design" and "Allowable Stress Design" of the AASHTO Guide Specifications of Horizontally Curved Bridges (AASHTO 1993) respectively:

Load Factor Design: $$\frac{D}{t_w} = \frac{36500}{\sqrt{F_y}}\left[1 - 4\frac{a}{R}\right] \le 192 \tag{2.6}$$

Allowable Stress Design: $$\frac{D}{t_w} = \frac{23000}{\sqrt{f_b}}\left[1 - 4\frac{a}{R}\right] \le 170 \tag{2.7}$$

Davidson et al. (1999) investigated the curvature effects on web panels under bending stress through finite element analysis. A "lateral pressure" analogy was developed to approximate the transverse displacement of the web panel. It was assumed that a lateral distributed load acts along the unit strip of the web due to curvature and non-collinearity. Figure 2.3 illustrates the applied stress based on the proposed analogy. The lateral pressure was given by:

$$q_c = \frac{p}{R} = \frac{\sigma t}{R} \tag{2.8}$$

where $q_c$ = lateral pressure due to curvature; $P$ = resultant tangential force due to curvature; $R$ = radius of curvature; σ = plate bending stress; and $t$ = panel plate thickness.

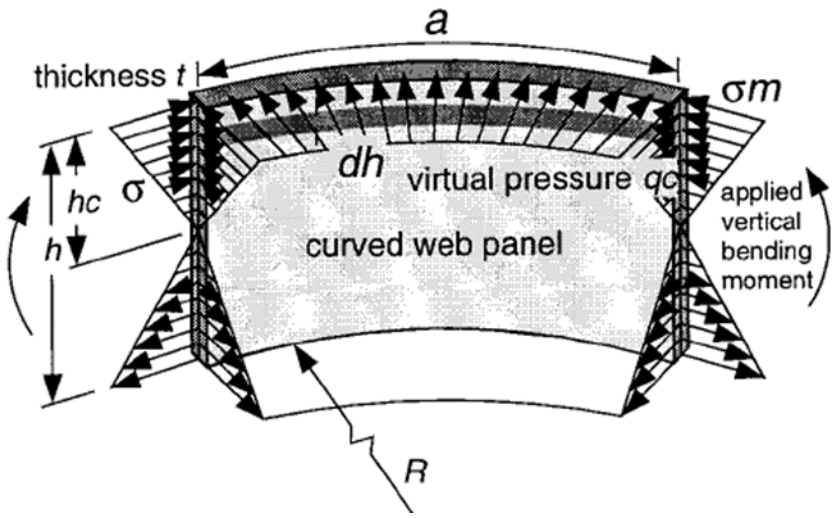


**Figure 2.3 Stresses on the girder as assumed in lateral pressure analogy (Davidson et. al 1999)**

Slenderness reduction factor for doubly symmetric non-composite curved girder was also defined as (Davidson, Ballance, and Yoo 1999):

$$\left[\frac{D}{t_w}\right]_{cv} \le \left[\frac{D}{t_w}\right]_{st} R_d \qquad (2.9)$$

where $R_d = 0.185\sqrt{\frac{R}{D}} \le 1.0$

## 2.4 V-Load Method

Horizontally curved bridges respond to loads differently than straight girders due to the torsional forces induced by the curvature. Richardson (1963) published a report explaining a simplified approximate method for analyzing horizontally curved bridges, which became known as the V-load method. In the V-load

approach, the torque produced by curvature is represented as a self-equilibrating load acting at the girder diaphragms, known as V-load. Thus, a curved girder is modeled as a straight girder and analyzed twice, once for the load acting on the girder and second time for the self-equilibrating V-load acting on the girder. The results of both of the analyses are then combined to obtain the demands.

Consider the horizontally curved bridge section shown in Figure 2.4. As can be seen, the girders in the unit are spaced at distance $D$. The radius of curvature of the outer and inner girders are $R_1$ and $R_2$, respectively. The diaphragms in the girder are spaced at distance $d$. The curvature of the unit is defined by $\theta$. The arc length of the outer and inner girder is given as $L_1$ and $L_2$.

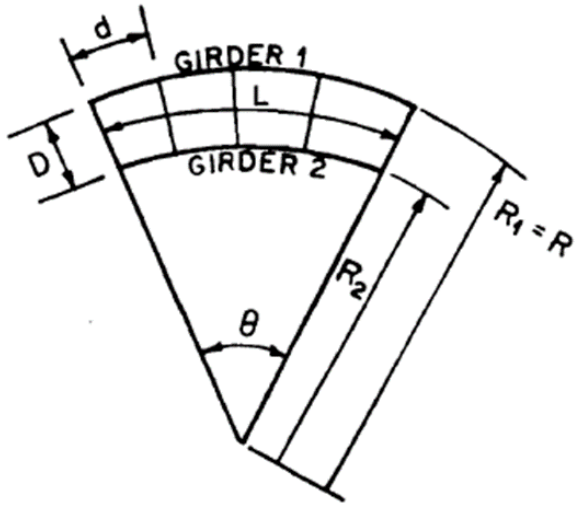


**Figure 2.4 Two curved girder system (Fiechtl et al. 1987)**

Bending moments due to vertical loads are resisted by the flanges and can be decomposed as longitudinal forces acting on the flanges. The longitudinal forces are represented by a force $M/h$ on the flanges of the girder in equal and opposite directions, as illustrated in Figure 2.5. Here $h$ is the distance between the flanges.

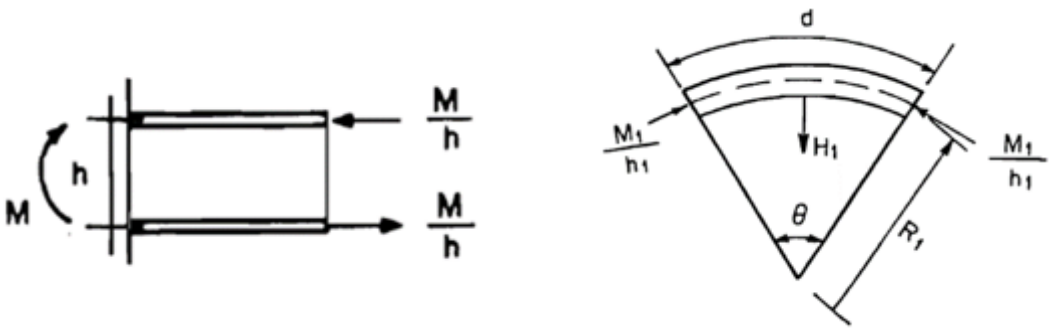


**Figure 2.5 (left) Equivalent forces due to moments; (right) resultant forces of top flange (Fiechtl et al. 1987)**

As shown in Figure 2.6**,** due to the horizontal curvature, the longitudinal forces due to bending are not in equilibrium and therefore it is not possible to calculate the demands on the girder due to static equilibrium. To maintain a radial equilibrium in the flange, a horizontal force ($H_1$) must be developed. This horizontal force develops along the diaphragm and is found by equilibrating along the radial line at the diaphragm location. The value of horizontal force acting on girder number one can be given as (Fiechtl, Fenves and Frank 1987):

$$H_1 = \frac{M_1 \theta}{h_1} \tag{2.10}$$

From geometry, θ can be given as $d/R$, and substituting into Equation 2.10 leads to:

$$H_1 = \frac{M_1 d_1}{h_1 R_1} \tag{2.11}$$

Similarly, this can be done for girder 2. Vertical shear is required for the equilibrium of the diaphragm, as shown in Figure 2.6.

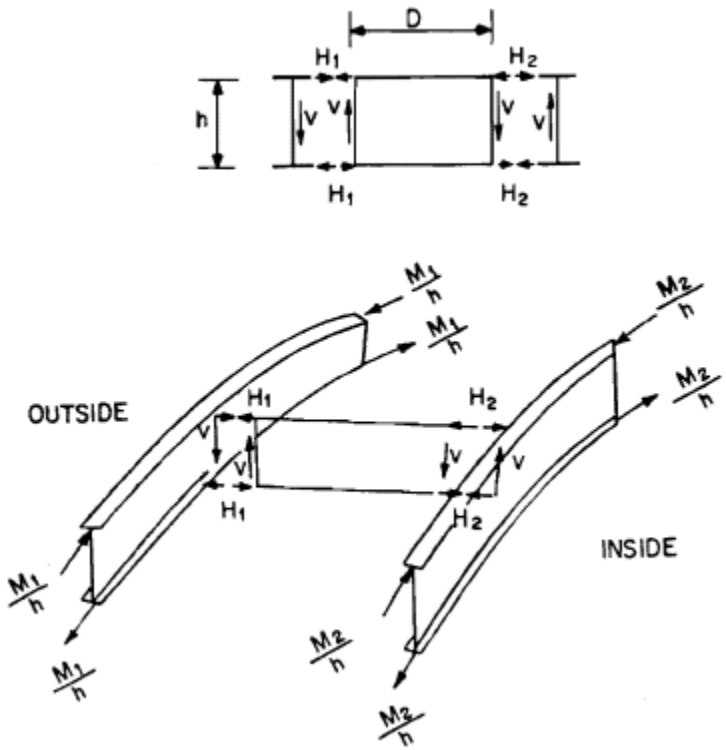


**Figure 2.6 Forces acting at the diaphragm location (Fiechtl et al. 1987)**

The vertical shear force acting along the girder can be calculated by taking moment equilibrium along any end of the diaphragm, which is given as:

$$V = (H_1 + H_2)\frac{h}{D} \tag{2.12}$$

By substituting the value of $H_1$ from Equation 2.11 and $H_2$ from an equivalent term for $H_2$ into Equation 2.12 leads to:

$$V = \frac{M_1 \frac{d_1}{R_1} + M_2 \frac{d_2}{R_2}}{D} \tag{2.13}$$

Considering $d_1 / R_1 = d_2 / R_2 = d / R$, the shear force is simplified as:

$$V = \frac{M_1 + M_2}{RD / d} \tag{2.14}$$

Figure 2.6 illustrates how these shear forces have opposite directions for each girder. The shear forces, so-called V-loads, approximate the curvature effect. It

should be noted that they are self-equilibrating since they are not external loads acting on the bridge. The total bending moments due to actual loads and forces developed by curved girder influence, V-loads, are denoted by $M_1$ and $M_2$ :

$$M_1 = M_{1P} + M_{1V} \tag{2.15}$$

$$M_2 = M_{2P} + M_{2V} \tag{2.16}$$

where subscript $P$ and $V$ represent the real loads and V-loads, respectively.

It has been proven that the bending moment due to V-load is small compared to moments resulting from external loads; therefore it is not included while calculating $M_1$ and $M_2$ (Fiechtl, Fenves, and Frank 1987). Thus, substituting the values of $M$ in equation 2.16, results in:

$$V = \frac{M_{1P} + M_{2P}}{RD/d} \tag{2.17}$$

A modified form of Equation 2.17 that can be used for applying the V-loads on multi-girder bridges is given by;

$$V = \frac{\sum_{i=1}^{N_g} M_{Pi}}{C(RD/d)} \tag{2.18}$$

where $M_{Pi}$ = primary girder moments; $N_g$ = number of girders; and $C$ = V-load coefficient given by Table 2.1.

**Table 2.1 V-Load coefficients (Fiechtl, Fenves, and Frank 1987)**

| Number of girders, $N_g$ | $C$ |
|---|---|
| 2 | 10000 |
| 3 | 10000 |
| 4 | 11111 |
| 5 | 12500 |
| 6 | 14000 |
| 7 | 15556 |
| 8 | 17143 |

Chapter 3

# Fatigue Assessment Methods

## 3.1 Introduction

Fatigue in metals is the initiation and growth of cracks under repetitive loading. This process can take place at stress levels that are substantially less than those associated with failure under static loading conditions (Fisher, Kulak, and Smith 1998). The fatigue damage process physically takes place in three phases, the crack initiation stage, crack propagation, and fracture phase (ASCE 1982). Due to the repetitive loading acting upon them through vehicles passing over every day, bridges are the most common civil engineering structures that are susceptible to fatigue.

Fillet welds have initial flaws such as partial penetration, porosity, undercut, etc. as illustrated in Figure 3.1. It has been proven that the fabrication flaws and stress concentrations due to structural misalignment are the main causes of fatigue crack initiation (Fisher, Kulak, and Smith 1998; Berge and Myhre 1977). The tensile stress component is the primary cause of crack propagation. Finally, the cracked section may fail due to reduced resistance under the cyclic load. Fatigue assessment methods have been developed for investigating the fatigue resistance and the remaining fatigue life of structures. This chapter presents standard fatigue assessment methods and explains residual stress effects on fatigue behavior.

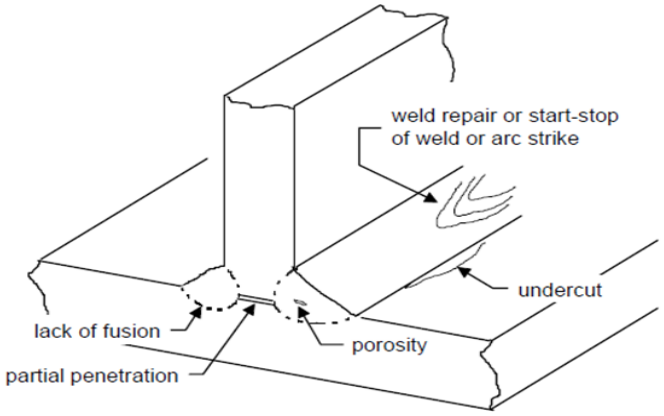


**Figure 3.1 Flaws in a fillet-welded detail (Fisher et al. 1998)**

### 3.2 Nominal-Stress Approach

S-N curves are the basis of fatigue assessment by the application of the nominal-stress method. The S-N curve represents the remaining fatigue life of fabrication detail versus stress range, as illustrated in Figure 3.2. The logarithmic scale is used for both axes. The S-N curves are provided in design codes based on fatigue test data under constant amplitude loading. It is assumed that the structural detail experiences infinite fatigue life if the stress range is below the Constant Amplitude Fatigue Limit (CAFL). The dashed lines in Figure 3.2 show the CAFL corresponding to each detail category.

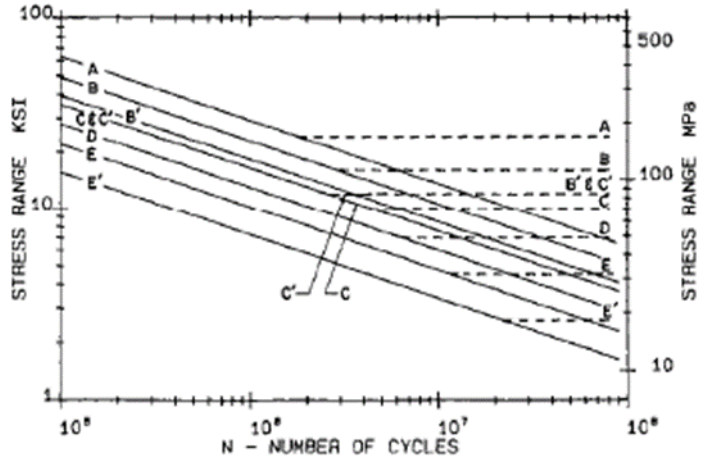


**Figure 3.2 AASHTO S-N curves for different detail categories (Grubb et al. 2015)**

The nominal-stress method is the most commonly used method for assessing the fatigue life of steel structures. Stress range, the difference between the maximum and minimum stress due to live load, is calculated near the weld using simple analysis. The remaining fatigue life in terms of loading cycles is related to the calculated stress range by the following equations:

$$NS^m = A \tag{3.1}$$

$$\log N = -m \log S + \log A \tag{3.2}$$

where $N$ = number of cycles; $S$ = stress range; $m$ = empirical material constants; and $A$ = detail category constants. It should be noted that $m$ is equal to the S-N curve slope and $A$ is chosen according to the corresponding detail category.

### 3.3 Hot-Spot Stress Approach

The hot-spot stress, local-stress method, is similar to the nominal-stress fatigue assessment method in terms of comparing the stress ranges with the corresponding S-N curve. The stresses are calculated locally at the weld toe of the weldments. Stress concentration effect related to weld geometry is considered in

the hot-spot method. The local-stress approach was developed initially for fatigue analysis of tubular joints of offshore structures (Marshall 2013). The hot-spot stress method is advantageous over the nominal-stress approach where the fatigue prone areas of a bridge structure with complex stress field, in-plane and out-of-plane stress combination, must be investigated (Grubb et al. 2015). There are two types of hot-spots related to weld geometry. As Figure 3.3 shows, type “a” is located on the plate surface, and type “b” is located on the plate edge.

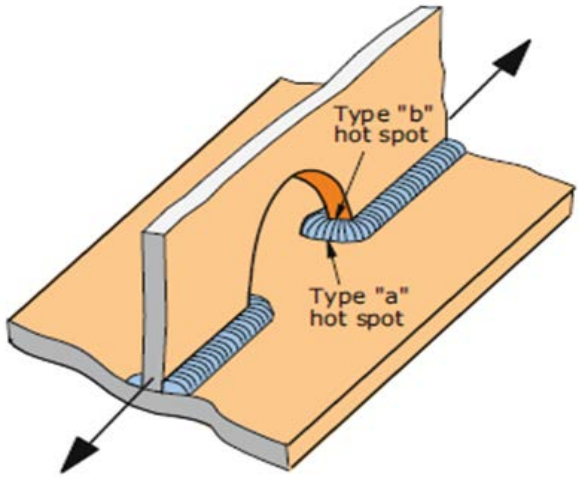


**Figure 3.3 Types of hot-spots (Niemi et al. 2018)**

The high stress gradient at hot-spots includes membrane stress, bending stress, and nonlinear stress peak due to weld notch. The nonlinear stress peak of the notch is not considered in finding the hot-spot stress, and the S-N curves include the notch stress effect instead. Extrapolation techniques are used in order to separate the membrane and bending stresses from the notch stress. These methods are applicable to stresses defined by measurement, experimental analysis, or finite element analysis. The linearization methods also depend on types of hot-spots, type “a” or “b.”

Sensors or strain gages must be installed at the reference points. The reference point locations depend on the type of hot-spots. Type “b” hot-spot remains the same through the plate thickness, while type “a” hot-spot stress changes through the plate thickness. Figure 3.4 illustrates the stress distribution

through the plate thickness for type “a” hot-spot. Equation 3.3 is used to calculate the type “a” hot-spot strain based on measured strain gages (Hobbacher 2016):

$$\varepsilon_{hs} = 1.67\varepsilon_A - 0.67\varepsilon_B \tag{3.3}$$

where $\varepsilon_A$ = strain from the gage located at 0.4$t$; $\varepsilon_B$ = strain from the gage located at 0.9$t$; and $\varepsilon_C$ = strain from the gage located at 1.4$t$.

The hot-spot stress can be defined by multiplying the elastic modulus of the welded plate, $E$, by the extrapolated hot-spot strain. In contrary to hot spot type “a”, stress distribution at the vicinity of weld toe related to type “b” hot spot is independent of plate thickness. Hence, extrapolation is done at three absolute distances from the weld toe. Type “b” hot-spot stress in terms of converted measured hot-spot strains into stresses is given by (Hobbacher 2016):

$$\sigma_{hs} = 3\sigma_{4mm} - 3\sigma_{8mm} + \sigma_{12mm} \tag{3.4}$$

where $\sigma_{4mm}$ , $\sigma_{8mm}$ , and $\sigma_{12mm}$ are stresses corresponding to measured strains at 4, 8, and 12 millimeters from weld toe, respectively.

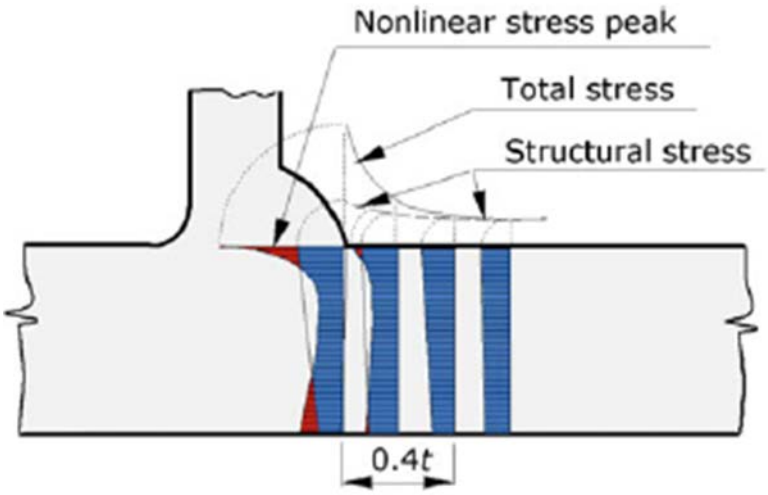


**Figure 3.4 Stress distribution through the depth of the welded plate (Hobbacher 2016)**

Hot-spot stresses can be determined by refined finite element analysis. However, the resulting hot-spot stress magnitudes are mesh dependent. Shell and

solid elements can be used for defining hot-spot stresses. The solid elements are more convenient in terms of modeling the weld geometry. Surface stress extrapolation is used for determining the hot-spot stresses at the weld toe. Reference points must be defined to extrapolate the finite element stresses similar to the reference points in the measurement method. The reference point locations depends on the mesh density and type of hot-spot under investigation (Niemi, Fricke, and Maddox 2018). Figure 3.5 illustrates the reference point locations for fine and coarse mesh densities related to each type of hot-spot “a” and “b”. The structural hot-spot stress can be calculated based on the following extrapolation equations (Hobbacher 2016).

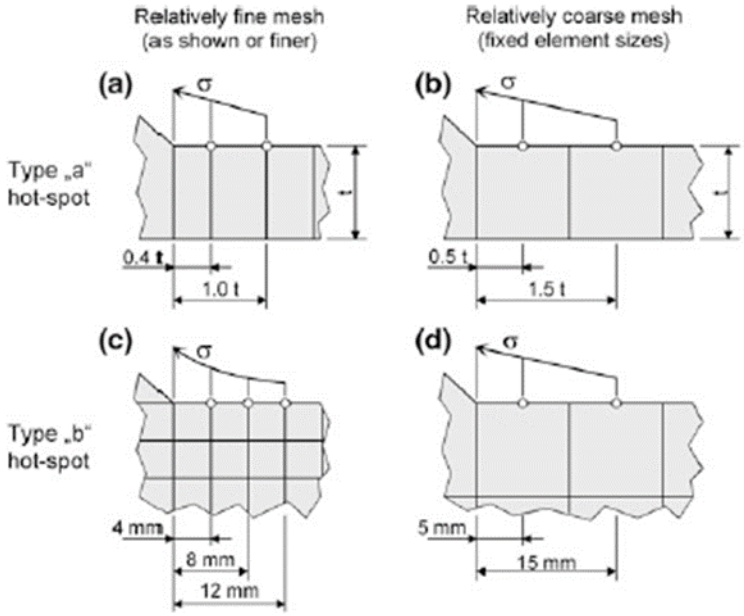


**Figure 3.5 Reference point definition or surface stress extrapolation (Hobbacher 2016)**

**Type “a” hot spot:**

For a fine mesh using element sizes less than 0.4$t$ with reference points located at 0.4$t$ and 1.0$t$, the linear extrapolation is given by:

$$\sigma_{hs} = 1.67\sigma_{0.4t} - 0.67\sigma_{1.0t} \tag{3.5}$$

For a fine mesh including element sizes less than 0.4$t$ with reference points located at 0.4$t$, 0.9$t$, and 1.4$t$, the quadratic extrapolation is given by:

$$\sigma_{hs} = 2.52\sigma_{0.4t} - 2.24\sigma_{0.9t} + 0.72\sigma_{1.4t} \quad (3.6)$$

For a coarse mesh, including higher-order elements having dimensions less than plate thickness, the extrapolation is as follows:

$$\sigma_{hs} = 1.50\sigma_{0.5t} - 0.5\sigma_{1.5t} \quad (3.7)$$

**Type "b" hot spot:**

For a fine mesh including element sizes less than 4 millimeters with reference points located at 4, 8, and 12 millimeters, the extrapolation is given by:

$$\sigma_{hs} = 3\sigma_{4mm} - 3\sigma_{8mm} + \sigma_{12mm} \quad (3.8)$$

For a coarse mesh including higher-order elements dimensioned less than 10 millimeters, the extrapolation is as follows:

$$\sigma_{hs} = 1.5\sigma_{5mm} - 0.5\sigma_{15mm} \quad (3.9)$$

### 3.4 Linear Elastic Fracture Mechanics (LEFM)

Fracture mechanics was first developed by Griffith (1921) to address the rupture of glass materials. The first structural engineering application of the method dates back to the 1940s for investigating the failure of ship hulls (Fisher, Kulak, and Smith 1998). Linear Elastic Fracture Mechanics (LEFM) is a well-known method for predicting the fatigue crack growth in linear elastic materials with initial cracks. The length of these small cracks is between 0.05 millimeters and 1 millimeter (Martinsson 2002).

The stress intensity factor (SIF) defines the state of stress at the crack tip. Analytical solutions have been developed for a limited number of crack configurations to find the stress intensity factor at the crack tip. The following expression can be used for cases in which the analytical solution is not available (Fisher, Kulak, and Smith 1998):

$$K = WY\sigma\sqrt{\pi a} \quad (3.10)$$

where $K$ = stress intensity factor; $W$ = constant related to the plate and crack geometry; $Y$ = constant related to crack tip stress field; and $a$ = crack length.

Similar to S-N curves for the nominal-stress fatigue assessment approach, fatigue crack growth ($da/dN$) can be plotted against stress intensity range ($\Delta K = K_{\max} - K_{\min}$). As Figure 3.6 illustrates, three regions correspond to two asymptotes $\Delta K_{th}$ and $\Delta K_C$. The first region represents the threshold region in which crack propagation is negligibly slow. It is noteworthy that the $\Delta K_{th}$ does not represent the $da/dN$ to be zero value; it corresponds to $4\times10^{-10}$ m/cycle according to ASTM-E647 (Farahmand, Bockrath, and Glassco 2012). The second region, the Paris region, is associated with the linear relationship between the crack growth rate and stress intensity range on a logarithmic scale. In the third region, crack growth occurs rapidly on the order of 0.01 mm/cycle until reaching the critical value (Schijve 2001). $K_C$ is defined by the stress intensity factor in which the materials fail. Different analytical approaches have been developed to determine the crack growth rate based on stress intensity ranges for the three regions of the crack propagation progress. Two prominent methods are described in the following.

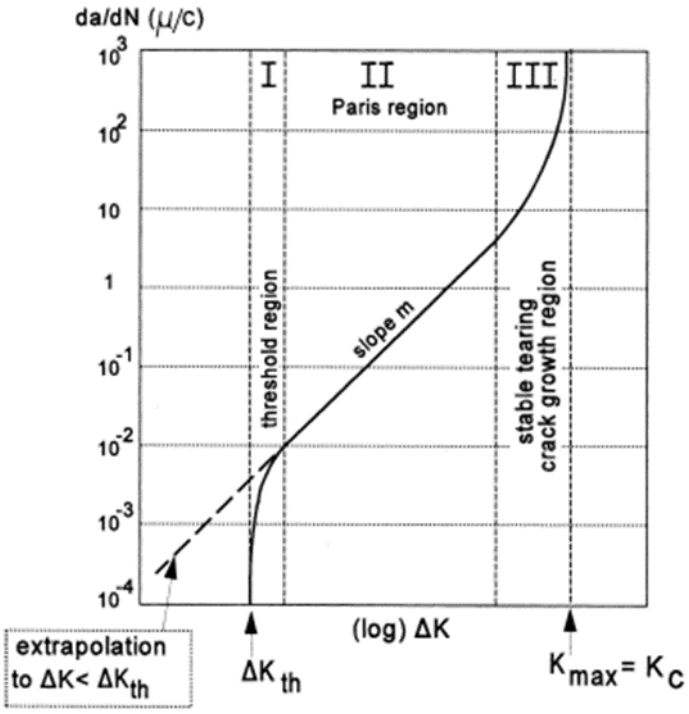


**Figure 3.6 Crack growth phases corresponding to stress intensity range (Schijve 2001)**

The most common expression used to relate the $da / dN$ and $K$ was first delveloped by Paris (1961) and therefore called the Paris Law given as:

$$\frac{da}{dN} = C\Delta K^m \tag{3.11}$$

where the $C$ and $m$ constants can be found by experimental data. The constant $m$ ranges from 3 to 5 and the constant $C$ values are between $10^{-10}$ and $10^{-6}$ (Farahmand, Bockrath, and Glassco 2012). The remaining fatigue life of the structure in terms of loading cycles can be determined by integrating Equation 3.12:

$$N = \frac{1}{C}\int_{a_i}^{a_f} \frac{1}{\Delta K^m} da \tag{3.12}$$

where $a_i$ and $a_f$ are initial and final crack lengths, respectively. As can be seen in Figure 3.6, the Paris Law is applicable to the second region where the variation of crack growth is linear with respect to stress intensity range. The asymptotic

behavior of the first and third region are not included in the Paris expression. Forman et al. (1967) proposed the following expression that includes the crack propagation behavior in the third region:

$$\frac{da}{dN} = \frac{C\Delta K^m}{(1-R)(K_C - K_{\max})} \tag{3.13}$$

where $R$ is the stress intensity ratio $K_{\min} / K_{\max}$.

### 3.5 Residual Stress

Residual stresses are unavoidable in built-up structural members that utilize welding to connect elements. Hence, a brief review of residual stress patterns and how residual stress is considered in fatigue analysis methods are given here. Generally, surface tensile residual stresses decrease fatigue performance by accelerating crack growth; however, compressive residual stresses may have a positive effect due to reducing the fatigue crack tip stresses (Webster and Ezeilo 2001). The sources of residual stresses in horizontally curved steel girders are welding, flame-cutting, and heat curving. Differential shrinkage during welding and thermal cutting leads to tensile and compressive residual stresses in heated and unheated areas, respectively (Russo et al. 2016). The measured residual stresses for three different grades of steel are shown in Figure 3.7. These stresses are related to residual stresses in the flanges of the welded plate girder parallel with the longitudinal axis of the beam. As can be seen in Figure 3.7, the highest magnitude of tensile residual stress occurs at the location of a web-to-flange fillet weld, and is equal to the yield stress.

Numerous analytical models have been proposed to define the residual stresses in welded structures (Chacón, Serrat, and Real 2012; Barth and White 1998; Clarin 2004; Taras 2010; Kim 2010). The two most commonly used residual stress models are related to The European Convention for Constructional Steelwork (ECCS 1976) and Culver and Nasir (1972). The ECCS model approximates the residual stresses due to flame cutting and welding, and the

Culver and Nasir model considers the heat curving residual stress in addition to welding and cutting residual stresses.

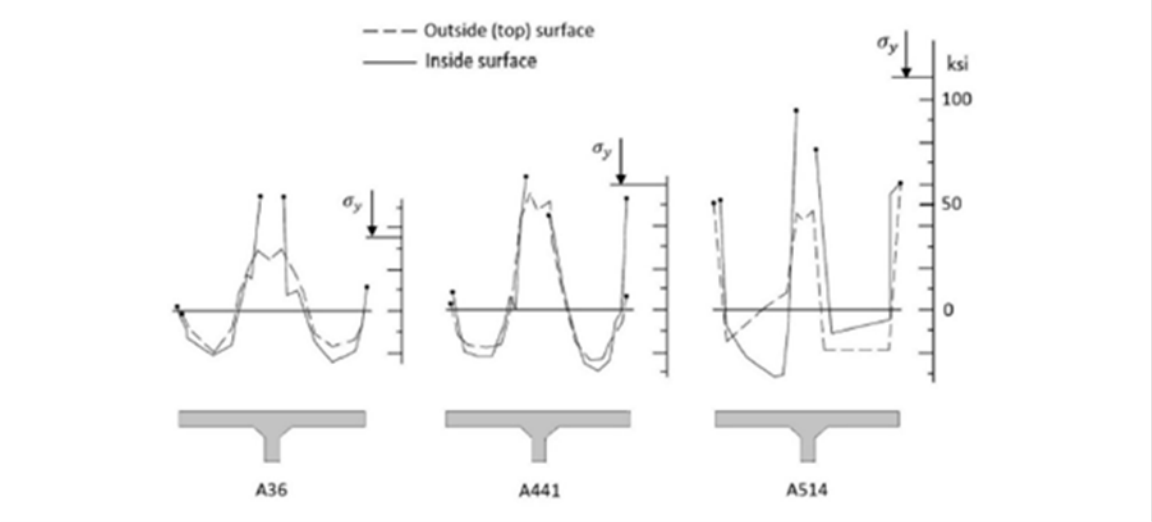


**Figure 3.7 Measured residual stress patterns (Fisher 1997)**

The ECCS (1976) method considers the residual stress to be a constant tensile value equal to the plate yielding stress at the heat-affected zones due to flame cutting and welding. The other zones that are outside of the tension zone are in compression and equilibrium with the resultant tensile forces. The tension block width at the flame-cut plate edge is given by:

$$C_f = \frac{1100\sqrt{t}}{F_y} \tag{3.14}$$

where $t$ = plate thickness in millimeters and $F_y$ = plate yield strength in MPa.
The tension width due to a single path of welding is as follows:

$$C_w = \frac{12000\,p(A_w)}{F_y\left(\sum t\right)} \tag{3.15}$$

where $p$ = efficiency factor (0.9 for the submerged arc welding process); $A_w$ = cross-sectional area of weld in ($mm^2$); $F_y$ = plate yield strength (MPa); and $\Sigma t$ = sum of the plate thicknesses meeting at the weld (mm). The combined effect of flame cutting and welding is determined by:

$$C_{fw}^4 = C_f^4 + C_w^4 \tag{3.16}$$

Figure 3.8 illustrates the residual stress pattern calculated by the ECCS model for an I-shaped section. The governing factor in S-N nominal and local stress fatigue assessment methods is the stress range that remains unchanged by adding the residual stress to the minimum and maximum stresses. Hence, residual stresses are not modeled explicitly when the reference S-N approach is applied in fatigue analysis. The effect of residual stress is included in the detail category fatigue resistance (Fisher et al. 1969). In another parametric study (Daniels and Batcheler 1979), the heat curving residual stress effect on fatigue strength of the curved steel girder was investigated. Two mechanisms were studied: mean stress effect and excessive web bowing under compressive residual stresses. It was concluded that “heat curving has no significant effect on the fatigue strength due to either mechanism.” In addition, it was recommended that the entire stress range, including the compressive stress, should be considered if any stress reversal occurs. Residual stresses are effective if the LEFM fatigue assessment method is applied. Residual stresses increase the crack tip stress intensity factor and changes stress intensity ratio, $R$.

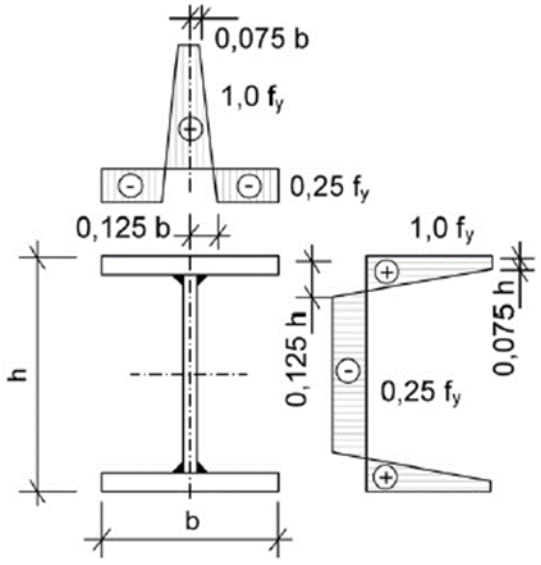


**Figure 3.8 ECCS (1976) residual stress pattern distribution (Pasternak et al. 2015)**

Chapter 4

# Special Fatigue Problem Mechanisms

There are a variety of fatigue problems related to steel bridges. These issues can be categorized based on the critical region under investigation, web or flange, bridge type, straight or curved girders, type of loading in a single girder panel, shear or bending, and the mechanisms in which fatigue cracks initiate. In the present chapter, the two most common fatigue mechanisms are reviewed: distortion induced fatigue and web breathing in slender girder webs. The experimental fatigue studies associated with curved girder systems are then presented and current design code limits addressing the reviewed fatigue mechanisms are given.

## 4.1 Distortion Induced Fatigue

Before the 1980s, it was a common practice not to attach the transverse stiffeners and connection plates to the tension flange to prevent brittle fatigue in the welded flange region. However, another severe fatigue problem appeared in the web-gap region between the short cut transverse stiffener and tension flange. In multi-girder steel bridges, lateral deflection of adjacent girders leads to rotation of the connection plate and distortion of a relatively flexible web gap region. The out-of-plane distortion of the web generates large stress concentrations at the toe of the transverse stiffener and causes fatigue cracking. This phenomenon is referred to as distortion-induced fatigue and accounts for the majority of fatigue cracks in bridges across the United States (Conner and Fisher 2006). Figure 4.1 illustrates the distortion-induced fatigue mechanism.

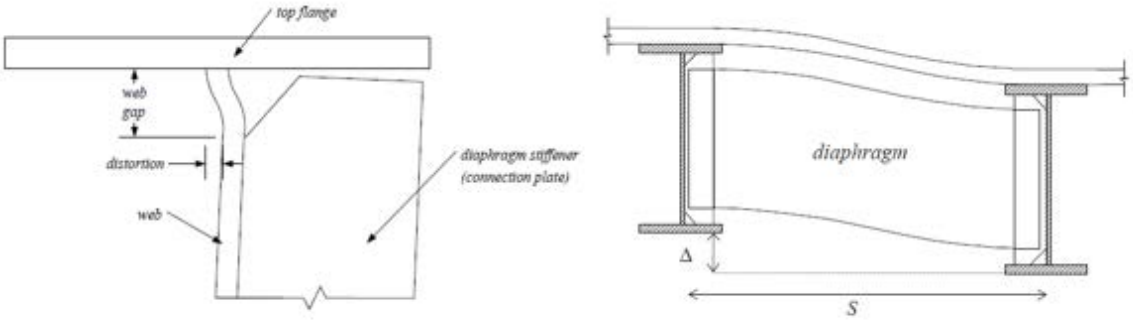


**Figure 4.1 Distortion induced fatigue (Li and Schultz 2005)**

Differing views have been presented on the critical regions in the bridge where the distortion-induced fatigue is most likely to occur. In a case study by Khalil et al. (1998), it was found that eight out of nine fatigue cracks occurred in the negative bending moment regions. In contrast, Roddis and Zhao (2001) suggested that differential deflections and out-of-plane bending moments are maximum in positive bending moment regions. Figures 4.2 and 4.3 show the distortion induced fatigue cracks in the lower and upper end of the connection plate, respectively.

**Figure 4.2 Fatigue cracks at lower end of the vertical connection plate (Bowman et al. 2012)**


**Figure 4.3 Fatigue cracks at upper end of the connection plate (Bowman et al. 2012)**

The major parameters affecting distortion-induced fatigue are lateral bracing system, web gap geometry, bridge geometry in terms of skew angle, span length, slab thickness, and girder spacing (Hassel et al. 2010). Berglund and Schultz (2006) conducted a parametric study on composite bridges by applying a linear finite element method to investigate the main factors affecting the adjacent girder differential deflections. They concluded that bridges with higher skew angles experience a greater differential deflection and maximum cross-frame deflections occur in the location of the obtuse corner of loaded lanes or at areas near the inflection points. It was also observed that long-span bridges, greater than 140 ft length, behave more uniformly due to composite action of the deck and undergo less differential deflections compared to short span bridges.

Barth and Bowman (2001) tested nine steel beams with welded diaphragms to investigate the failure modes and strength of the diaphragm-to-beam connection. It was found that staggered diaphragm systems have a better performance in reducing the fatigue cracks developed at the location of the bottom flange-to-web connection compared to the non-staggered diaphragms. However, it was concluded by Grondin et al. (2000) that staggered cross-frame configurations are more susceptible to fatigue cracking in comparison with the non-staggered configurations.

Distortion-induced cracks initially propagate parallel to the major bending axis in the longitudinal direction; hence fatigue failures can be prevented by early retrofitting (Fisher 1984). Generally, retrofitting methods for avoiding fatigue distortion is based on two approaches: (1) stiffening fatigue prone details to minimize distortion, and (2) softening or increasing the flexibility of the system. Diaphragm removal is another method that can be used to mitigate distortion-induced fatigue in bridges; however, this does not apply to curved girder bridges due to the primary role of diaphragms in minimizing warping and rotations.

### 4.2 Web Breathing

When slender plate girders are designed based on post-buckling resistance, large out-of-plane deformations can be induced under in-plane loading. The repeated web buckling deformation, which is known as “web breathing,” leads to fatigue cracks under cyclic loading (Günther and Kuhlmann 2004). Inevitable initial imperfections and residual stresses lead to out-of-plane deformations under loads less than theoretical buckling loads (Crocetti 2003). Figure 4.4 illustrates the breathing mechanism in which buckling deformations lead to high secondary-bending stresses that causes fatigue cracks in the web.

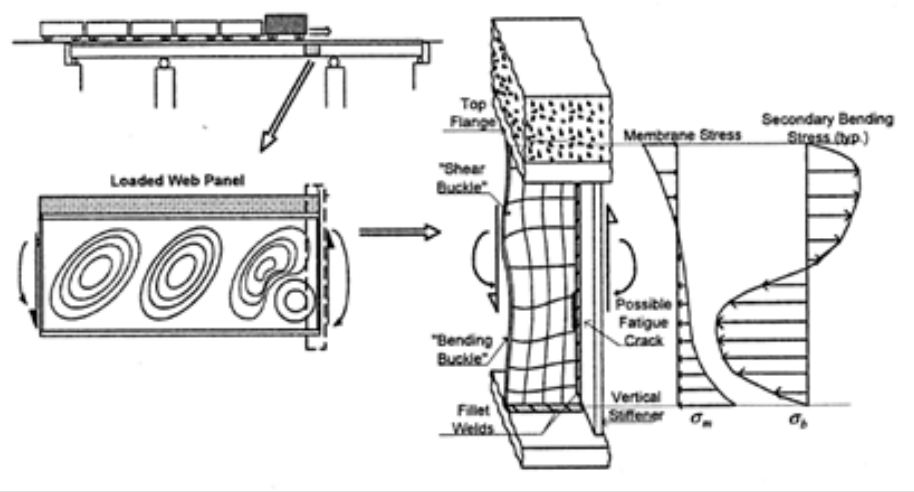


**Figure 4.4 Web breathing effect for a slender composite bridge girder (Crocetti 2001)**

Web breathing fatigue has been investigated through analytical and numerical (FEM) studies to quantify the parameters affecting the web boundary stresses (Duchene and Maquoi 1998; Maeda and Okura 1983; Davies and Roberts 1996; Okura, Yen, and Fisher 1993; Remadi, Aribert, and Raoul 1995; Spiegelhalder 2000). It was indicated that the main parameters that affect geometric stresses resulting from web breathing are panel aspect ratio and slenderness ratio, stiffness of boundary members, form, and magnitude of initial out-of-plane deflections (geometric imperfections).

Various experimental tests on slender girders with web breathing indicated that the fatigue cracks could be classified based on the type of loading and place of origin (Spiegelhalder 2000; Roberto Crocetti 2001; Yen and Mueller 1966; Toprac and Natarajan 1971) as illustrated in Figure 4.5. The characteristics of each crack type are as follows:

- **Type 1** cracks occur at the toe of the weld connecting the compression flange to the web (Okura, Yen, and Fisher 1993). Repeated out-of-plane web deformations caused by secondary bending stresses (web breathing) under in-plane bending results in the fatigue crack initiation (Crocetti 2001). The crack initiated at the weld toe propagates at a relatively slow rate at the

web side of the girder under mixed modes 1 and 3 related to tension and tearing conditions, respectively (Roberts and Davies 2002).

- **Type 2** cracks occur at the weld toe on the web side of the transverse stiffener connection to the web (Crocetti 2001). Tensile membrane bending stresses below the neutral axis results in the propagation of the crack under tension mode into the tension flange and may lead to failure (Roberts and Davies 2002). Type 2 cracks propagate at a faster rate compared to Type 1 cracks due to the fact that the tensile membrane stresses are more significant than the secondary bending stresses (Crocetti 2001).
- **Type 3** cracks occur due to fillet weld discontinuities at the weld toe connecting the web to the tension flange. Type 3 cracks are not associated with web breathing.
- **Type 4** cracks occur at the weld toe corners where the diagonal tension field buckling displacements are anchored when a panel is under shear loading (Okura, Yen, and Fisher 1993). Type 4 cracks propagate in the direction of weld toes and eventually through the web where high local shear deformations and plate bending stresses exist (Crocetti 2001). The breathing nature of the crack follows the Type 1 crack propagation rate and mode combinations (Roberts and Davies 2002).
- **Type 5 and 6** cracks occur at the weld connecting the web to load-carrying transverse stiffener near the neutral axis of the girder (Roberts and Davies 2002). A part of the applied concentrated load is carried by the web region welded to the transverse stiffener that results in reduced web flexural stiffness and, consequently, large out-of-plane web deformations (Crocetti 2001). This mechanism causes fatigue crack propagation along the web to stiffener weld toe and through the web.

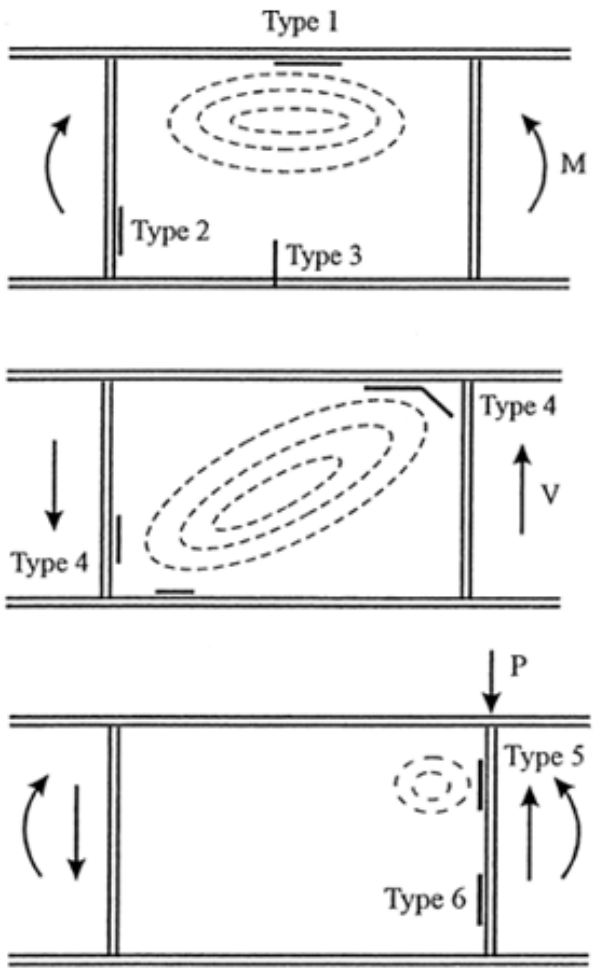


**Figure 4.5 Fatigue cracks locations in slender webs corresponding to loading conditions (Roberts and Davies 2002)**

### 4.3 Curved Girder Fatigue Research Review

There are very limited studies specifically on the fatigue behavior of curved steel girders. The only available sources found by the authors are Daniels and Herbein (1980) at Lehigh University and Nakai et al. (1990) in Japan. Both research approaches and findings are discussed in the following.

In 1973, a multiphase project entitled “Fatigue of Curved Steel Bridge Elements” was funded by FHWA to investigate the fatigue problems related to horizontally curved steel bridges. The project phases were: 1) analysis and design of curved I-girder and box girders; 2) special studies such as residual stress, heat

curving, and diaphragm spacing; 3) fatigue test experiments; 4) investigation of ultimate strength of the test assemblies; and 5) final design recommendations based upon the findings (Daniels and Herbein 1980). The proposed slenderness ratio equations and the effect of residual stresses were explained in sections 2.2 and 3.5 of the present report, respectively. Phase 3 of the project, which includes the fatigue experiments of horizontally curved I-girders are discussed briefly here.

Five different weld detail categories were considered, and five twin-girder assemblies were fabricated to investigate each detail type fatigue behavior. As can be seen in Figure 4.6, the assemblies consisted of two girders connected by five X-type diaphragms with a 120 ft centerline radius of curvature. Two loading conditions with 2 million constant amplitude cycles were applied at the assemblies: 1) loading at quarter points of each girder web; and 2) loading at the middle space between the quarter points of the girders. Assemblies were monitored during loading cycles for two fatigue cracking mechanisms: 1) primary cracking due to in-plane bending and torsion; and 2) secondary fatigue cracks due to out-of-plane web plate bending. Geometric specifications associated with each assembly are given in the Table 4.1.

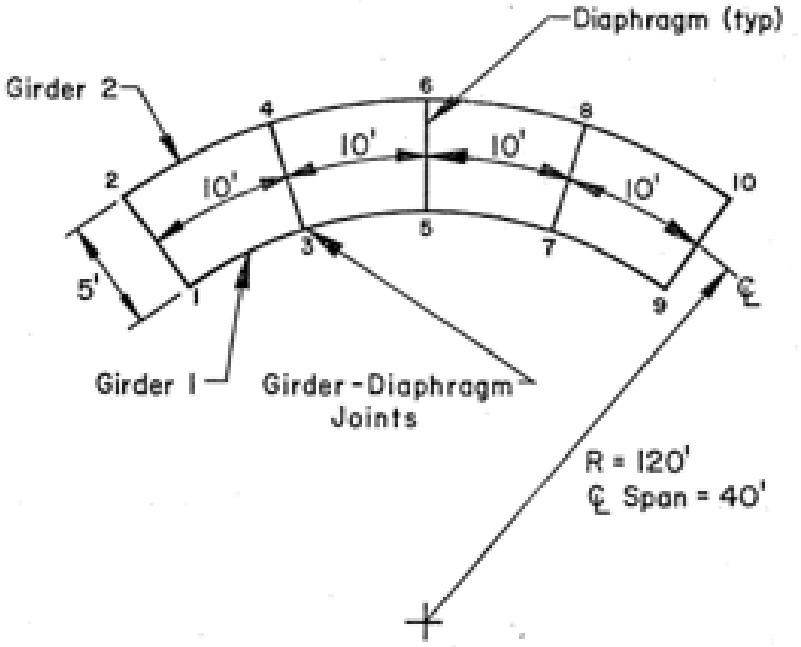


**Figure 4.6 Schematic plan view of test girders (Daniels and Herbein 1980)**

**Table 4.1 Summary of cross section dimensions (Daniels and Herbein 1980)**

| Assembly | Girder | Flange width (inch) | Flange Thickness (inch) | Web Depth (inch) | Web Thickness (inch) | Slenderness Ratio |
|---|---|---|---|---|---|---|
| 1 | 1 | 12 | 1 | 54 | 3/8 | 144 |
| | 2 | 12 | 1 | 54 | 9/32 | 192 |
| 2 | 1 | 8 | 1/2 | 58 | 3/8 | 155 |
| | 2 | 10 | 3/4 | 58 | 5/16 | 186 |
| 3 | 1 | 8 | 1/2 | 58 | 3/8 | 155 |
| | 2 | 10 | 3/4 | 58 | 3/8 | 155 |
| 4 | 1 | 8 | 1/2 | 52 | 3/8 | 139 |
| | 2 | 12 | 1 | 52 | 3/8 | 139 |
| 5 | 1 | 8 | 1/2 | 52 | 3/8 | 139 |
| | 2 | 12 | 1 | 52 | 3/8 | 139 |

After evaluating the fatigue cracks of each assembly, it was concluded that the straight girder fatigue strength associated with each detail category is acceptable to be used for fatigue analysis of curved girders. Although fatigue cracks initiated at the web gap between the transverse stiffener and bottom flange, no fatigue cracks were observed at the web boundaries connecting to the flanges and stiffeners.

Nakai et al. (1990) conducted an experimental study to investigate the fatigue strength of fillet welds at the web boundaries of horizontally curved girders. The research consisted of two parts: 1) developing analytical equations to approximate the out-of-plane bending stress and displacement, and 2) fatigue testing the fabricated curved girders up to failure. In their approach, the curved web plate was idealized as a strip beam model loaded by the equivalent lateral force acting on the web. The out of plane bending stress was then estimated using

elementary beam theory. The developed equations were used to run a parametric study to determine the test models' geometries to maximize the stresses at the web boundary fillet joints. Five singly supported curved girders were loaded under pure bending, as can be seen in Figure 4.7.

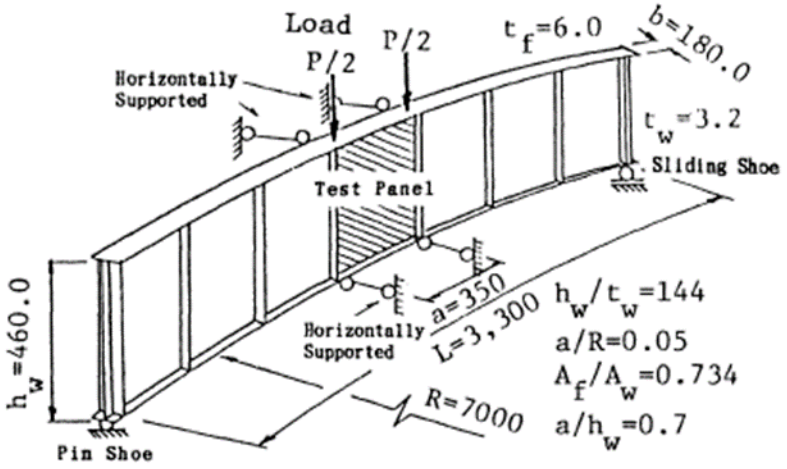


**Figure 4.7 Test girder configuration (Nakai et al. 1990)**

It was observed that fatigue cracks propagated at the locations between the transverse stiffener and compression flange and at the tension flange where horizontal supports restrained the lateral displacement. However, no fatigue cracks occurred at the fillet welds connecting the web to the flange plates.

## 4.4 Current Design Limits

### AASHTO Specification

There are two fatigue categories defined in AASHTO (2017): (1) load-induced and (2) distortion-induced fatigue. In the load-induced fatigue category, AASHTO limits the web shear force to shear buckling resistance of the web by Equation 4.1:

$$V_u \leq V_{cr} \tag{4.1}$$

Where $V_u$ is the shear in the web at the section under consideration due to the unfactored permanent load plus the factored fatigue load (kip) and $V_{cr}$ is shear-

buckling resistance. It is assumed that the member sustains infinite fatigue life related to elastic flexing of the web. In the distortion-induced part, the problem is addressed through proper detailing, and no further limit is mentioned.

**Eurocode Specifications**

The Eurocode (2006) limits the web slenderness by Equation 4.2 to prevent web breathing fatigue in road bridges:

$$\frac{b}{t} \leq 30 + 4L \leq 300 \tag{4.2}$$

where $b$ is the web height, $t$ is the web thickness, and $L$ is the span length in meters and is assumed to be greater than 20 meters. It should be noted that both specifications limits are related to slender straight girders, and none of them provide guidance specifically to curved steel webs.

Chapter 5

# Finite Element Analysis

## 5.1 Model Geometry

The finite element analysis studies were conducted using the commercial FEM software package ABAQUS (2019). Two modeling strategies were utilized to capture the stress ranges corresponding to different fatigue crack types that are developed in slender curved girders. The girder specifications are given in Table 5.1.

**Table 5.1 Geometry used in finite element analyses**

| $t_w$ (in) | $D$ (in) | $t_f$ (in) | $b_f$ (in) | $d_o$ (in) | $L_b$ (ft) | $R$ (ft) | Span Length (ft) | Slenderness ratio |
|---|---|---|---|---|---|---|---|---|
| 0.4 | 120 | 1.35 | 24 | 120 | 30 | 900 | 240 | 300 |

### Loading Condition:

The AASHTO (2017) fatigue truck was used for the loading configuration. The fatigue truck is similar to the HL-93 design truck, but the axis spacings is fixed at 14 and 30 feet. Axis loads must be increased by 15 percent to consider the dynamic effects after girder distribution factors were applied. Yellow arrows on Figure 5.2 define the load positions.

### Boundary Conditions:

A cylindrical coordinate system was defined to apply the boundary conditions. The R, T, and Z axis correspond to the radial direction normal to the

web, the longitudinal direction tangent to the web, and vertical direction along the web, respectively. The curved girder is assumed to be simply supported, hence all the nodes at the left flange bottom were restrained for translation in 3 directions, and the nodes related to right flange bottom were restrained for translation in vertical and radial directions. A set of nodes at the top and bottom of transverse stiffeners were defined to apply the lateral bracing effect. The radial translation associated with the set was restrained. Orange arrows in Figure 5.1 represent the boundary condition positions.

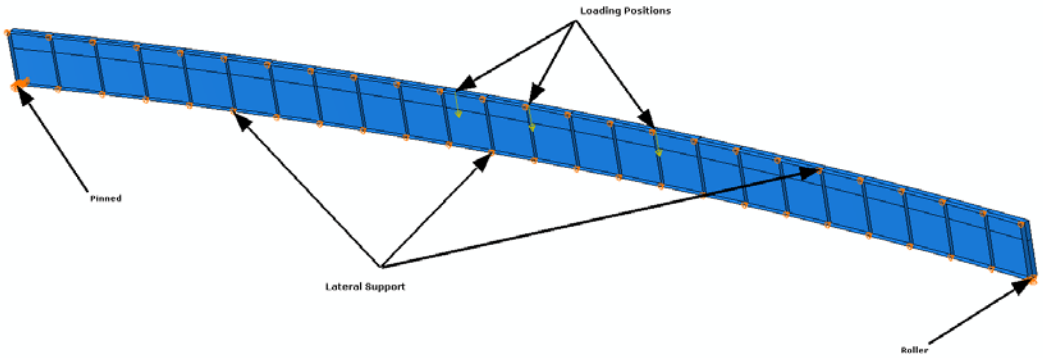


**Figure 5.1 Load and boundary positions**

## 5.2 Modeling Strategies

### 5.2.1 Web Boundary Fatigue Investigation Approach

The most influential parameter related to the web breathing of slender girders is the initial imperfection of the web. In order to impose the initial geometric imperfections into analysis, the following two step procedure was followed. First, a linear buckling analysis was conducted to extract mode shapes. The buckling mode shape related to the first eigenvector is shown in Figure 5.2. The magnitude of the deformations are normalized output values and can be scaled to fit the allowed limits. Bridge welding code (2010) web distortion tolerance limits were applied in which the maximum web initial out of flatness was set to $d$/80. Second, the scaled buckling mode shapes were used as the initial geometry to run a geometrically nonlinear analysis under the same loading. The ABAQUS (2019)

S4R shell elements, having 6 DOF's per node with reduced integration, were used to model the web, transverse stiffeners, flanges, and longitudinal stiffeners.

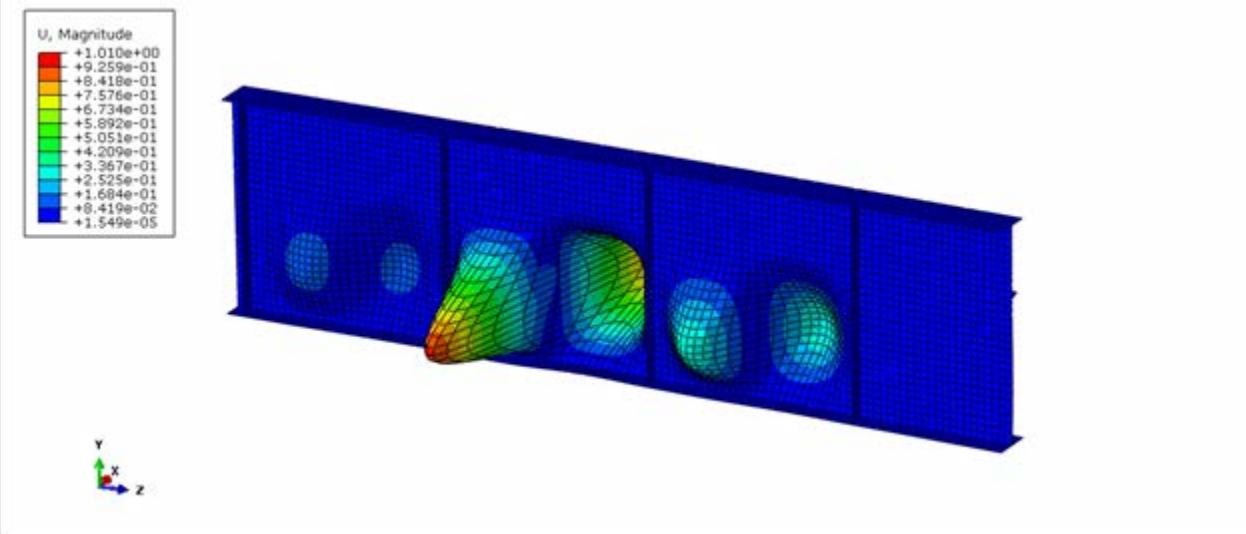


**Figure 5.2 First buckling mode shape**

### 5.2.2 Fatigue Investigation Approach at the Lateral Support Locations

There is a complex stress state at the connection between the transverse stiffener and flange and web elements. The lateral displacements in the radial direction are restrained at those locations. The bending moment and rotation of the tension flange are the primary causes of the stress complexity. Moreover, the connection details and weld geometry make it more challenging to get an accurate stress state at the connection location. Hence, a two-level analysis referred to as the sub-modeling technique was applied. In the first step, all girder parts are modeled using S4R shell elements in the global model. In the second step, a sub-model of the critical region is regenerated using solid elements, C3D8R, and displacements from the global shell model are applied at the boundary of the sub-model. This method optimizes the computational cost by using shell elements for global analyses and results in accurate stress definitions due to solid element capabilities. Figure 5.3 shows the submodel and global model geometry. A very fine mesh of dimensions approximately equal to 0.25 inch for each element was used to precisely calculate the complex stress state due to lateral bracing and detailed weld geometry. Figure 5.4 shows the submodel mesh and weld geometry.

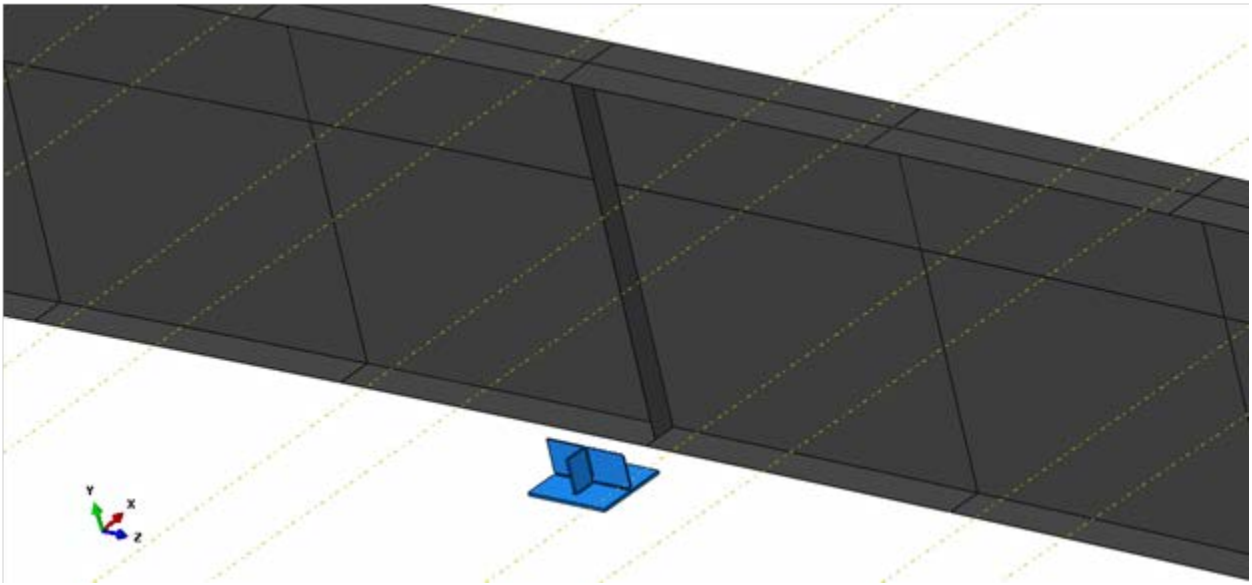

**Figure 5.3 Global model and submodel**

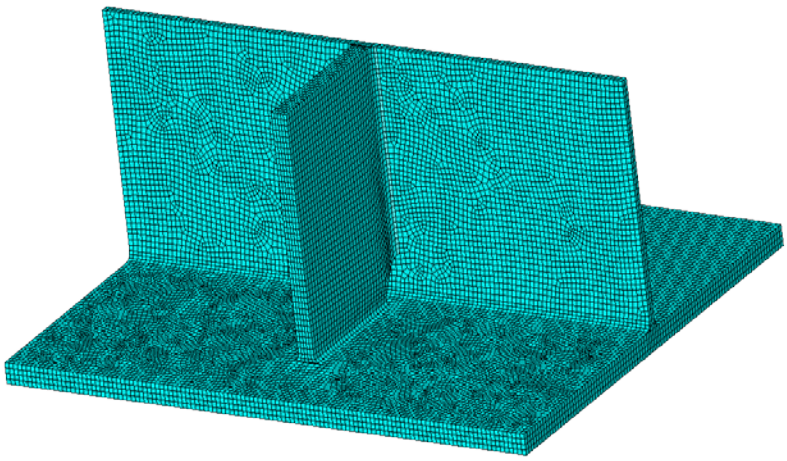

**Figure 5.4 Submodel mesh density**

## 5.3 FEM Results

### 5.3.1 Web Boundary Fatigue Investigation

Nominal-stress fatigue assessment was used to compare the stress ranges with the nominal fatigue strength corresponding to each fatigue prone location. First, the web connection to the top flange area was considered. As explained in section 4.2, fatigue cracks such as Type 1 and 4 may develop because of the web breathing at the top flange region. The web stresses perpendicular to the top flange causes the possible fatigue cracks to initiate. Figure 5.5 shows the vertical stresses of the critical panel. The stresses near the top flange are in the order of 2 ksi. The fatigue strength of breathing webs is equal to 16 ksi (Günther 2002; Crocetti 2001). The stress range (2 ksi) being much less than the fatigue strength indicates that the fatigue cracks will not likely occur at the web to top flange connection. The small web normal stresses at the top flange location is the result of the longitudinal stiffener effect in mitigating the lateral deformations of the web. As Figure 5.5 shows, the web normal stresses at the bottom flange are much larger (almost 10 ksi) compared to the top flange stresses due to the significant initial imperfections.

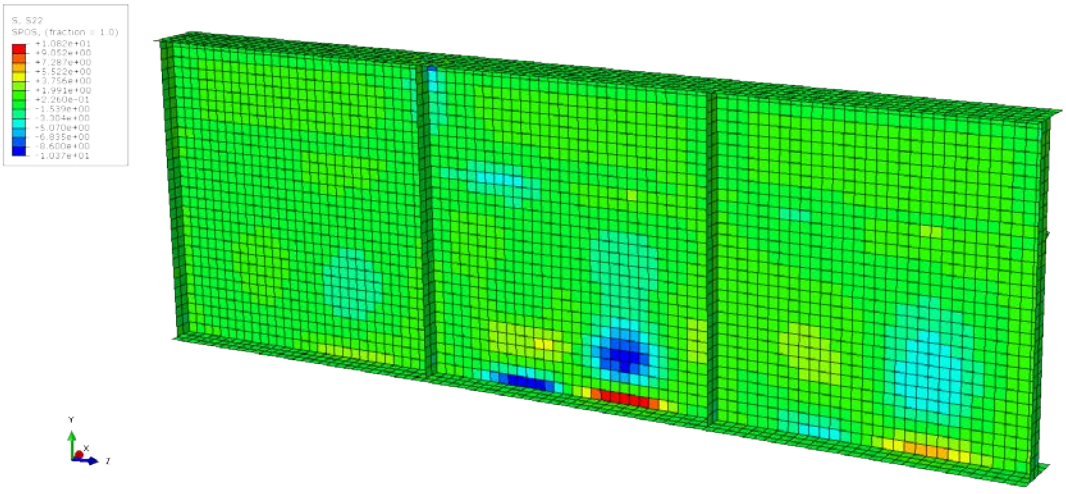

**Figure 5.5 Web stresses in vertical direction (ksi)**

Type 5 fatigue cracking might occur at the web to bottom flange connection if the bending stresses in the longitudinal direction of the girder exceed the corresponding fatigue strength of the detail. Figure 5.6 represents the tangential

stress distribution along the longitudinal axis of the girder. The maximum stress is equal to 15.8 ksi. The fatigue strength of the bottom flange to web connection is defined by AASHTO (2017) Detail B category, which is equal to 16 ksi. Hence, the web connection to the bottom flange region is more susceptible to fatigue cracking due to bending stresses along the girder rather than the web transverse stresses normal to the bottom flange. The last location to check for the possible crack initiation (Types 4, 5, and 6) is the transverse stiffener connection to the web region. The stress range close to the middle of the web at the transverse stiffener location is less than 1 ksi, and the stress range close to the bottom of the transverse stiffener and web is less than 11 ksi. Hence, Type 4, 5, and 6 cracks may not develop considering the corresponding fatigue strength of 16 ksi.

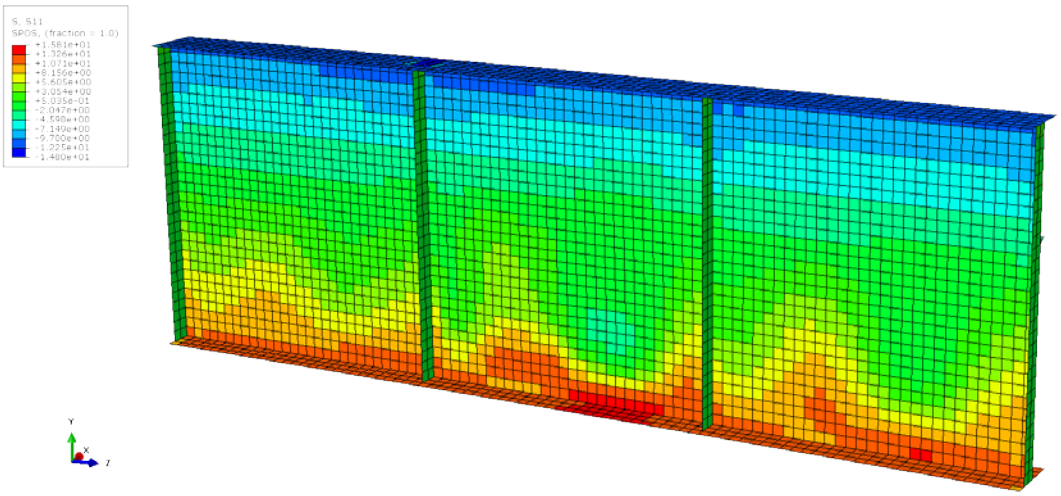

**Figure 5.6 Tangential (longitudinal) stress distribution (ksi)**

### 5.3.2 Fatigue Investigation at the Lateral Support Locations

Hot-spot stress fatigue assessment was applied to determine the fatigue crack initiation potential at the transverse stiffener connection to the web where the lateral support conditions were imposed. Russo et al. (2016) recommended using AASHTO detail category C and stress measured at the 0.25 inch of the weld toe when the hot-spot stress method is applied. Figure 5.7 shows the tangential stress distribution at the submodel with the high stress concentration just above the transverse stiffener weld. Tangential stress at the node 0.25 inch away from

the weld toe is almost 30 ksi, which is much larger than the 10 ksi fatigue resistance corresponding to detail category C. Hence, fatigue cracks are likely to occur at the lateral bracing connection to the transverse stiffener.

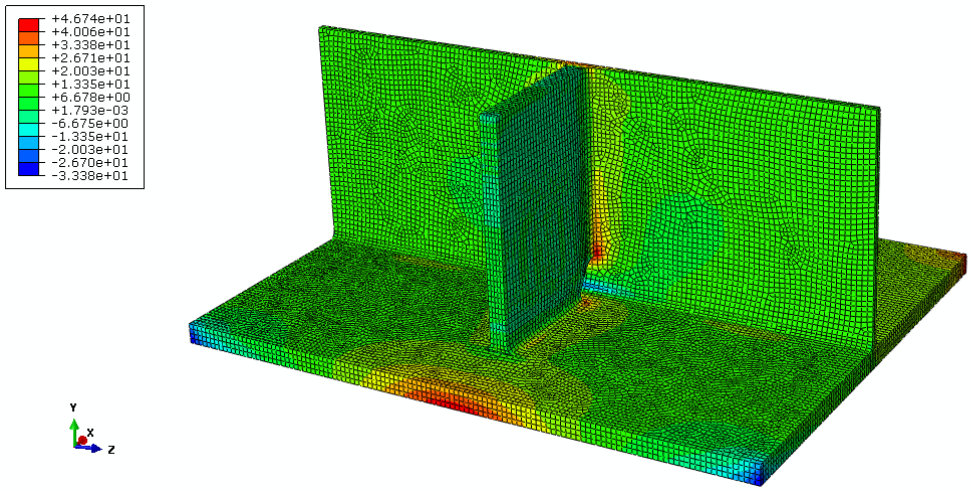


**Figure 5.7 Tangential stress, longitudinal, distribution of submodel (ksi)**

Chapter 6

# Summary and Conclusions

Horizontally curved steel bridges are advantageous over curved concrete bridges because of their lightweight and ability to facilitate longer spans. Erection and construction of curved steel girders require less time compared to concrete bridges, which is a significant factor considering the expenses of closing the highways for building new ramps or flyovers. However a deep understanding of curved girders' complex mechanics is required for the strength design of these structures, and fatigue problems associated with curved girder systems must be addressed for the longterm performance of the bridge. This study focused on fatigue behavior of horizontally curved steel bridges.

Researches at the national level have been conducted in the U.S. since late 1960’s to develop the strength limits of curved girder systems and specifications for designers. The Consortium of University Research Teams (CURT) and Curved Steel Bridge Research Project (CSBRP) were the two most significant projects in developing the curved girder design specifications based on analytical and experimental studies for ultimate strength limit design. In contrast, very limited researches have been done to investigate the fatigue design considerations associated with curved girder bridges.

The most common type of fatigue problem in U.S. bridges is associated with differential lateral deflection of the adjacent girders in multi-girder bridges, which is referred to as distortion induced fatigue. It is estimated that more than 90 percent of fatigue cracks in the U.S. occur due to the distortion induced fatigue phenomenon. The small web gap between the cut short transverse stiffener and

flange experiences large stress concentrations applied by the rotation of connecting elements such as floor beams and diaphragms connection plates. Connecting the transverse stiffener end to the flange at the lateral cross-frame locations is the most effective way to prevent distortion induced fatigue.

Another fatigue problem associated with slender girders is caused by “web breathing.” Web breathing fatigue is defined by fatigue cracks that result from the repeated out-of-plane deformations of the web of slender girders. This problem has been studied widely for straight girders in European countries since the 1990s. Web slenderness limits based on bridge span length are provided by the Euro code to control web breathing.

The only fatigue study of curved steel girders in the U.S. was conducted in 1973 entitled “Fatigue of Curved Steel Bridge Elements”. The multi-phase project investigated the residual stresses effect on the fatigue performance of curved girders. Five twin girder assemblies were fatigue tested. It was concluded that the fatigue cracks do not occur at the web panel boundaries with slenderness ratio up to 192, however fatigue cracks were observed at the diaphragm connection points to the web.

In another study in Japan in 1990, single curved girders were fatigue tested until failure. No fatigue cracks were observed in the web boundaries of the test girders. However, fatigue cracks initiated at the lateral support locations used for stabilizing the curved web panels.

A FEM model of a slender curved girder was built based on AASHTO (2017) and analyzed for different fatigue crack types. Two modeling strategies were applied to capture the possible fatigue crack initiation in the curved girder. Initial imperfections were imposed as scaled buckling mode shapes, and the nominal-stress fatigue assessment method was used to evaluate the fatigue performance at web boundaries. It was concluded that fatigue cracks are unlikely to occur at the web to top flange connection. The longitudinal stiffener restrains the top web lateral deformations, and the resulting stress at the top flange weld to the web are consequently small. The bottom flange connection to the web is susceptible to

fatigue cracking due to high longitudinal bending stresses. However, the stresses due to web deformation at the bottom flange regions are less than the fatigue resistance of the detail.

A sub-modeling simulation technique was applied to investigate the web performance at the transverse stiffeners connection to the bottom flange where the lateral displacements were restrained. The hot-spot stress fatigue assessment method was used to evaluate the fatigue performance of the region. The calculated hot-spot stress was higher than the corresponding fatigue strength. Hence, there is the potential that fatigue cracks will occur at the web to transverse stiffener connection near the bottom flange. In general, based on the reviewed experimental studies related to the fatigue of curved girders and the FEM simulation of the present study, it can be concluded that the highest fatigue prone areas in slender-web curved girders are located at the web near the bottom flange and the bottom of transverse stiffeners.

Based on the literature review and finite element modeling the following future work is recommended:

- Use refined three-dimensional finite element analysis for capturing the complex stress state at diaphragm connection plate of slender curved girders.
- Investigate strengthening the connection at the lateral bracing to prevent possible fatigue cracking at web.
- Investigate multi-girder curved assemblies to quantify the composite deck and cross-frame forces effect on fatigue performance.
- Conduct field studies to verify the stress state in curved steel bridge girders from fabrication, erection, and service.

# REFERENCES


ABAQUS. 2019. http://www.3ds.com

AASHTO. 1992. “Standard Specifications for Highway Bridges, ASD and LFD.” American Association of State Highway and Transportation Officials, 15th ed. Washington, D.C.

AASHTO. 1993. “Guide Specifications for Horizontally Curved Highway Bridges”, as revised in 1981, 1982, 1984, 1985, 1986, 1990, and 1992, American Association of State Highway and Transportation Officials Washington, D.C.

AASHTO, LRFD. 2017. “AASHTO LRFD Bridge Design Specifications.” American Association of State Highway and Transportation Officials, 8th Ed. Washington, DC.

ASCE. 1982. “ASCE Committee on Fatigue and Fracture Reliability.” Fatigue Reliability: Journal of Structural Division, 3–23.

AWS (American Welding Society), 2010. *Bridge Welding Code*. AASHTO/AWS D1. 5M/D1. 5: 2010.

Barth, Karl E., and Donald W. White. 1998. “Finite Element Evaluation of Pier Moment-Rotation Characteristics in Continuous-Span Steel I Girders.” Engineering Structures 20 (8): 761–78.

Berge, S., and H. Myhre. 1977. “Fatigue Strength of Misaligned Cruciform and Butt Joints.” Norwegian Maritime Research 5 (1).

Bowman, M. D., G. Fu, Y. E. Zhou, R. J. Connor, and A. A. Godbole. 2012. “NCHRP Report 721: Fatigue Evaluation of Steel Bridges.” Washington, DC.

Chacón, R., M. Serrat, and E. Real. 2012. “The Influence of Structural Imperfections on the Resistance of Plate Girders to Patch Loading.” *Thin-Walled Structures* 53 (April): 15–25.

Clarin, Mattias. 2004. “High Strength Steel: Local Buckling and Residual Stresses.” Doctoral dissertation, Luleå tekniska universitet.

Connor, Robert J., and John W. Fisher. 2006. “Identifying Effective and Ineffective Retrofits for Distortion Fatigue Cracking in Steel Bridges Using Field Instrumentation.” *Journal of Bridge Engineering* 11 (6): 745–52.

Crocetti, Roberto. 2001. On Some Fatigue Problems Related to Steel Bridges. PhD Dissertation, Chalmers University of Technology.

Culver, C. G., and N. Nasir. 1969. “Instability of Horizontally Curved Members, Flange Buckling Studies.” Report submitted to the Pennsylvania Department of Highways by Department of Civil Engineering Carnegie-Mellon University, Pittsburgh.

Culver, C. 1972. “Design Recommendations for Curved Highway Bridges.” Final Report for Research Project 68-32. Pennsylvania Department of Transportation, Harrisburg, Pa.

Culver, Charles G., Clive L. Dym, and Tasnim Uddin. 1973. “Web Slenderness Requirements for Curved Girders.” *Journal of the Structural Division* 99.

Daniels, J. H., and R. P. Batcheler. 1979. “Fatigue of Curved Steel Bridge Elements - Effect of Heat Curving on The Fatigue Strength of Plate Girders,” No. FHWA-RD-79-135 Intrm Rpt.

Daniels, J. H., and W. C. Herbein. 1980. “Fatigue of Curved Steel Bridge Elements - Fatigue Tests of Curved Plate Girder Assemblies.” Rep. No. FHWA-RD-79-133, Lehigh Univ., Bethlehem, Pa., 157.

Davidson, James S., Scott R. Ballance, and Chai H. Yoo. 1999. “Finite Displacement Behavior of Curved I-Girder Webs Subjected to Bending.” *Journal of Bridge Engineering* 4 (3): 213–20.

Davidson, James S., and Chai H. Yoo. 1996. “Local Buckling of Curved I-Girder Flanges.” *Journal of Structural Engineering* 122 (8): 936–47.

Davidson, James S., and Chai H. Yoo. 2000. “Evaluation of Strength Formulations for Horizontally Curved Flexural Members.” *Journal of Bridge Engineering* 5 (3): 200–207.

ECCS. 1976. *Manual on Stability of Steel Structures 2nd Edition*. European Convention for Constructional Steelwork.

Farahmand, Bahram, George Bockrath, and James Glassco. 2012. *Fatigue and Fracture Mechanics of High Risk Parts: Application of LEFM & FMDM Theory*. Springer Science & Business Media.

Fiechtl, A. L., G. L. Fenves, and K. H. Frank. 1987. “Approximate Analysis of Horizontally Curved Girder Bridges.” Final Report No. FHWA/TX-91+ 360-2F.

Fisher, John W. 1997. “Evolution of Fatigue-Resistant Steel Bridges.” Transportation Research Record 1594 (1): 5–17.

Fisher, John W., Karl Heinz Frank, Manfred A. Hirt, and Bernard M. McNamee. 1969. “Effect of Weldments on the Fatigue Strength of Steel Beams.” Final Report, Fritz Laboratory Reports. Paper 323, September 1969 (70-25).

Fisher, John W., Jian Jin, D. C. Wagner, and B. T. Yen. 1990. “Distortion-Induced Fatigue Cracking in Steel Bridges,” NCHRP Report 336, Transportation Research Board, National Research Council, USA.

Fisher, John W., Geoffrey L. Kulak, and Ian FC Smith. 1998. “A Fatigue Primer for Structural Engineers.” National Steel Bridge Alliance, American Institute of Steel Construction.

Forman, Royce G., V. E. Kearney, and R. M. Engle. 1967. “Numerical Analysis of Crack Propagation in Cyclic-Loaded Structures.” *Journal of Basic Engineering* 89, 459–464.

Galambos, Theodore V. 1978. *Tentative Load Factor Design Criteria for Curved Steel Bridges*. Research Report No. 50, Washington University, School of Engineering and Applied Science, Department of Civil Engineering.

Griffith, Alan Arnold. 1921. “VI. The Phenomena of Rupture and Flow in Solids.” Philosophical Transactions of the Royal Society of London. Series A, Containing Papers of a Mathematical or Physical Character 221 (582–593): 163–98.

Grubb, Michael A., Kenneth E. Wilson, Christopher D. White, and William N. Nickas. 2015. “Load and Resistance Factor Design (LRFD) for Highway Bridge Superstructures - Reference Manual.” National Highway Institute (US).

Günther, HP. 2002. “Ermüdungsverhalten von Stahlträgern Mit Schlanken Stegblechen Im Brückenbau. Universität Stuttgart, Mitteilungen Des Instituts Für Konstruktion Und Entwurf, Nr. 2002-1.” PhD Dissertation, February 2002.

Hobbacher, Adolf. 2016. *Recommendations for Fatigue Design of Welded Joints and Components* 2nd edition. Springer International Publishing. ISBN 978-3-319-23756-5.

Hartmann, J.L. 2005. “An Experimental Investigation of the Flexural Resistance of HorizontallyCurved Steel I-Girder Systems.” dissertation submitted to the faculty of the Graduate School of the University of Maryland, College Park, MD.

Kim, Yoon Duk. 2010. “Behavior and Design of Metal Building Frames Using General Prismatic and Web-Tapered Steel I-Section Members.” PhD Dissertation, Georgia Institute of Technology.

Linzell, D., D. Hall, and D. White. 2004. “Historical Perspective on Horizontally Curved I Girder Bridge Design in the United States.” *Journal of Bridge Engineering* 9 (3): 218–29.

Li, Huijuan, and Arturo E. Schultz. 2005. "Analysis of girder differential deflection and web gap stress for rapid assessment of distortional fatigue in multi-girder steel bridges." Final Report 2005-38, Minnesota Department of Transportation, St. Paul, MN (MN/RC-2005-38).

Marshall, Peter William. 2013. *Design of Welded Tubular Connections: Basis and Use of AWS Code Provisions*. Developments in Civil Engineering Vol. 37 Elsevier.

Martinsson, J. 2002. “Fatigue Strength of Welded Cruciform Joint with Cold Laps.” Design and Analysis of Welded High Strength Steel Structures, 163–84.

Nakai, Hiroshi, Toshiyuki Kitada, Hiroshi Ishizaki, and Katsuyoshi Akehashi. 1990. “An Experimental Study on Fatigue Strength of Web Plates for Horizontally Curved Plate Girders.” Doboku Gakkai Ronbunshu, no. 416: 125–33.

Niemi, Erkki, Wolfgang Fricke, and Stephen J. Maddox. 2018. “Structural Hot-Spot Stress Approach to Fatigue Analysis of Welded Components.” IIW Doc 13: 1819–00.

Okura, Ichiro, Ben T. Yen, and John W. Fisher. 1993. “Fatigue of Thin-Walled Plate Girders.” Structural Engineering International 3 (1): 39–44.

Pasternak, H., B. Launert, and T. Krausche. 2015. “Welding of Girders with Thick Plates — Fabrication, Measurement and Simulation.” *Journal of Constructional Steel Research* 115 (December): 407–16.

Paris, Paul C. 1961. “A Rational Analytic Theory of Fatigue.” *The Trend in Engineering* Vol 13, pp.9-14.

Richardson, Gordan. 1963. “Analysis and Design of Horizontally Curved Steel Bridge Girders, United States Steel Structural Report.” ADUSS 88-6003-01.

Roberts, T. M, and A. W Davies. 2002. “Fatigue Induced by Plate Breathing.” *Journal of Constructional Steel Research* 58 (12): 1495–1508.

Russo, Francesco M., Dennis R. Mertz, Karl H. Frank, and Kenneth E. Wilson. 2016. “Design and Evaluation of Steel Bridges for Fatigue and Fracture–Reference Manual.” National Highway Institute (US).

Saint-Venant, Barré de. 1843. “Mémoire Sur Le Calcul de La Résistance et de La Flexion Des Pieces Solides Asimple Ou Adouble Courbure, En Prenant Simultanément En Consideration Les Divers Efforts Auquels Elles Puevent Êntre Soumise Dans Touts Les Sens.” CR Acad Sci Paris 17 (942): 1020–31.

Schijve, Jaap. 2001. *Fatigue of Structures and Materials*. Springer Science & Business Media.

Schuenzel, Peter F. 1982. “Strength of Horizontal Curved Plate Girders.” PhD Dissertation, Lehigh University.

Stegmann, T. H., and T. V. Galambos. 1976. “Load Factor Design Criteria for Curved Steel Girders of Open Section.” Research Report No 43. Washington University.

Taras, Andreas. 2010. “Contribution to the Development of Consistent Stability Design Rules for Steel Members.” Ph.D. dissertation, Graz University of Technology.

Webster, G.A., and A.N. Ezeilo. 2001. “Residual Stress Distributions and Their Influence on Fatigue Lifetimes.” *International Journal of Fatigue* 23: 375–83.

Ziemian, Ronald D. 2010. *Guide to Stability Design Criteria for Metal Structures*. John Wiley & Sons.